

Search for (sub)stellar companions of exoplanet hosts by exploring the second ESA-Gaia data release

K.-U. Michel^{1,*} & M. Mugrauer¹

¹*Astrophysikalisches Institut und Universitäts-Sternwarte Jena, Schillergäßchen 2, D-07745 Jena, Germany*

Correspondence*:

Corresponding Author: K.-U. Michel
kai-uwe.michel@uni-jena.de

ABSTRACT

We present the latest results of an ongoing multiplicity survey of exoplanet hosts, which was initiated at the Astrophysical Institute and University Observatory Jena, using data from the second data release of the ESA-Gaia mission. In this study the multiplicity of 289 targets was investigated, all located within a distance of about 500 pc from the Sun. In total, 41 binary, and 5 hierarchical triple star systems with exoplanets were detected in the course of this project, yielding a multiplicity rate of the exoplanet hosts of about 16 %. A total of 61 companions (47 stars, a white dwarf, and 13 brown dwarfs) were detected around the targets, whose equidistance and common proper motion with the exoplanet hosts were proven with their precise Gaia DR2 astrometry, which also agrees with the gravitational stability of most of these systems. The detected companions exhibit masses from about 0.016 up to 1.66 M_{\odot} and projected separations in the range between about 52 and 9555 au.

Keywords: Multiple Stars, White Dwarfs, Brown Dwarfs, Exoplanets, ESA-Gaia DR2

1 INTRODUCTION

Since the detection of the first planet orbiting a star other than the Sun, several thousands of these exoplanets have been discovered by various detection techniques. While the majority of stars are members of multiple star systems (Duchêne and Kraus, 2013), most of the exoplanet host stars are single stars. Nevertheless several multiple star systems hosting exoplanets, could already be revealed by previous multiplicity studies using seeing limited or high contrast AO imaging observations (see e.g. Mugrauer et al., 2014; Mugrauer and Ginski, 2015). In order to explore the effects of the presence of stellar companions on the formation process and orbital evolution of exoplanets, a survey was initiated at the Astrophysical Institute and University Observatory Jena (described in detail by Mugrauer, 2019) to identify and characterize companions of exoplanet host stars, detected in the second data release of the European Space Agency (ESA) Gaia mission (Gaia DR2 from hereon, Gaia Collaboration et al., 2018). Furthermore, in Mugrauer and Michel (2020) a comparable investigation was carried out among potential exoplanet host stars, identified by the TESS mission (Ricker et al., 2015). The study, whose results are presented here, is the third work in the context with Mugrauer (2019). The following section gives a detailed description of this study, and the detected companions and their derived properties are presented in the third section of this paper.

2 GAIA DR2 SEARCH FOR (SUB)STELLAR COMPANIONS OF EXOPLANET HOSTS

The Gaia DR2, is based on data taken by the Gaia spacecraft in the first 22 months of its mission and contains 1.7 billion detected sources up to a limiting magnitude of $G = 21$ mag. For 1.3 billion sources a five parameter astrometric solution could be derived, i.e. beside their equatorial coordinates (α, δ), also the parallax π and proper motion ($\mu_\alpha \cos(\delta), \mu_\delta$) of these sources were determined. Furthermore, for about 88 million detected objects estimates of their G-band extinction and effective temperature are listed in the Gaia DR2, determined by the Priam algorithm, which is part of the astrophysical parameters inference system (Apsis, see Bailer-Jones et al., 2013) in the Gaia data processing.

Using Gaia DR2 data Mugrauer (2019) already explored the multiplicity of all exoplanet host stars, whose exoplanets were detected either by photometric transit observations, radial-velocity (RV), or astrometric measurements, and were listed in the *Extrasolar Planets Encyclopaedia*¹ (EPE from hereon, Schneider et al., 2011) by mid of October 2018. The study, presented in this paper, complements this survey by investigating the multiplicity of the exoplanet hosts (stars but also brown dwarfs), whose planets were indirectly detected either via RV measurements or transit observations in the range of time between mid of October 2018 until end of September 2020, as well as all exoplanet hosts, known so far, with planets, which were directly detected by imaging observations. At the end of September 2020 the EPE lists about 4350 exoplanets, and about 400 of them were detected around the hosts studied in this work.

(Sub)stellar Companions are expected to be located at the same distance to the Sun as the exoplanet hosts and form common proper motion pairs with them, in particular wide companions with projected separations of hundreds and thousands of au, i.e. the typical targets of this study. Hence, in order to clearly detect such companions and to prove the equidistance of these objects and the exoplanet hosts, in this study we have taken into account only Gaia DR2 sources with an accurate five parameter astrometric solution, i.e. which exhibit precise measurements of their parallax ($\pi/\sigma(\pi) > 3$) and proper motion ($\mu/\sigma(\mu) > 3$). Thereby, sources with negative parallaxes are neglected. As in the Gaia DR2 a parallax uncertainty of 0.7 mas is reached for faint sources down to $G = 20$ mag, the survey is furthermore constrained to exoplanet hosts, which are located within a distance of 500 pc around the Sun (i.e. $\pi > 2$ mas), to assure $\pi/\sigma(\pi) > 3$ even for the faintest companions, detectable in this survey. This distance constraint is slightly relaxed to $\pi + 3\sigma(\pi) \gtrsim 2$ mas, i.e. taking into account also the parallax uncertainty of the hosts. By the end of September 2020, in total 289 exoplanet hosts are listed in the EPE, which fulfill this distance constraint, and hence are selected as targets for this study. The properties of all targets are summarized in Tab. 1 and their histograms are illustrated in Fig. 1. On average, the targets are solar like stars most frequently found within 150 pc around the Sun, which exhibit proper motions in the range between about 2 and 10400 mas/yr, and G-band magnitudes from about 3.7 to 20.8 mag. In particular, the sub-sample of direct imaging exoplanet hosts emerges as a peak in the age distribution at young ages, as all these targets are typically younger than 0.1 Gyr, in contrast to hosts of RV and transiting exoplanets, which are older than 1 Gyr in general.

The companion search radius, applied in this project around the selected targets, is limited to a maximal projected separation of 10000 au, which guarantees that the majority of wide companions of the exoplanet hosts are detectable in this study, as described by Mugrauer (2019). This upper separation limit results in an angular search radius around the targets of $r[\text{arcsec}] = 10\pi[\text{mas}]$. Within this radius around the targets the companionship of all sources, listed in the Gaia DR2 with an accurate five parameter astrometric solution was investigated. For the verification of the equidistance of all detected sources with the associated

¹ Online available at: <http://exoplanet.eu/>

exoplanet hosts, the difference $\Delta\pi$ between their parallaxes was calculated, taking into account also the excess noise of their astrometric solutions. Common proper motion of the detected sources and the targets was checked with the precise Gaia DR2 proper motions of the exoplanet hosts μ_{PH} and the sources μ_{Comp} . In addition, we have also derived for all sources the differential proper motion: $\mu_{rel} = |\mu_{PH} - \mu_{Comp}|$, which yields the common proper motion index (cpm-index = $|\mu_{PH} + \mu_{Comp}|/\mu_{rel}$), which characterizes the degree of common proper motion of the detected sources and the exoplanet hosts.

Following the companion identification procedure ($sig\text{-}\Delta\pi \leq 3$ & cpm-index ≥ 3), as defined by Mugrauer (2019) the majority of all sources (>99.88 %), detected within the applied search radius around the targets, can clearly be excluded as companions, as they are either not located at the same distances as the exoplanet hosts and/or do not share a common proper motion with them. In contrast, for 61 detected objects their companionship with the targets could clearly be proven with their precise Gaia DR2 astrometry. For all these companions we have determined their relative astrometry to the exoplanet hosts (angular separation ρ , and position angle PA), as well as their projected separation sep , derived with their angular separation and the parallax of the targets.

The absolute G-band magnitude of all companions was derived from their apparent G-band photometry, the parallax of the associated exoplanet hosts, as well as their Apsis-Priam G-band extinction estimate, all listed in the Gaia DR2. If there was no extinction estimate given for a companion, the extinction estimate of the exoplanet host was used instead or if not available, its extinction estimate, listed in the *StarHorse* catalog (Anders et al., 2019). In the case that no G-band extinction is available at all it was derived from V-band extinction measurements of the exoplanet hosts, listed either in the *VizieR* data base² (Ochsenbein et al., 2000) or in the literature, adopting $A_G/A_V = 0.77$, as described by Mugrauer (2019).

The masses and effective temperatures of all detected companions were determined from their derived absolute G-band magnitudes using the evolutionary models of (sub)stellar objects from Baraffe et al. (2015), as well as the ages of the exoplanet hosts, as listed in the *EPE*. Thereby, we adopt the same age for the planet hosts and their companions. We determined the masses and effective temperatures of the companions via interpolation of the model grid with the age closest to that of the exoplanet hosts. For verification of the obtained results the properties of the companions derived from their G-band magnitudes were compared with those, determined from the near-infrared photometry, taken from the 2MASS Point Source catalogue (Skrutskie et al., 2006), if available. For the near-infrared extinction we have used the relations: $A_{Ks}/A_V = 0.12$, $A_H/A_V = 0.17$, and $A_J/A_V = 0.26$, as described in Mugrauer (2019). A graphical comparison of the masses obtained from the G-band and the 2MASS photometry are shown in Fig. 2. The identity is illustrated as grey dashed line in this figure. For all companions the derived masses agree well with each other, with deviations that remain below the 3σ level (the same holds also for the temperature estimates not shown here). Objects, whose masses were determined by extrapolation from the used model grids as such as those with bad quality (quality flags all but A) or contaminated 2MASS photometry were excluded in this comparison.

Eventually for all companions, which were detected in this study, we have estimated their escape velocity $\mu_{esc} [mas\ yr^{-1}] = 2\pi\sqrt{2M\pi_{PH}^3/\rho}$ with their angular separation ρ and the parallax of the associated exoplanet hosts both in the unit of milli-arcsec (mas), as well as the total mass M of the system (in the unit M_\odot), i.e. the sum of the mass of the companions, derived as describe above, and the mass of the associated

² Online available at: <https://vizier.u-strasbg.fr/>

exoplanet hosts, taken from the EPE. This estimation can be considered as an upper limit of the escape velocity as the projected separation is smaller than the physical separation of the objects.

3 DETECTED COMPANIONS OF EXOPLANET HOSTS

The Gaia astro- and photometry of all exoplanet hosts and their companions, detected in this study, are listed in Tab. 2. The derived properties of the companions are summarized in Tab. 3 to 5. In all tables the exoplanet host systems or the companions are sorted by their right ascension. The used identifier of the targets corresponds either to the one used in the EPE or is a slightly abbreviated version of it. In contrast to the planet definition used by the EPE, in which substellar objects below $60 M_{Jup}$ are defined as exoplanets, we follow here the planet definition based on the deuterium burning limit (as described e.g. by Basri, 2000), i.e. all substellar objects below $13 M_{Jup}$ are classified as exoplanets, while more massive objects below the substellar/stellar mass limit (at about $0.072 M_{Jup}$ for solar metallicity) as brown dwarfs, respectively. Thereby the given masses of the exoplanets, detected by radial velocity measurements, correspond to minimum-masses ($M \sin(i)$) due to the unknown orbital inclination, while masses of direct imaging planets are usually derived from their spectrophotometry with evolutionary models.

In Tab. 2 for each exoplanet host and its detected co-moving companion(s) their Gaia DR2 parallax π , proper motion in right ascension and declination ($\mu_\alpha \cos(\delta)$ & μ_δ), astrometric excess noise (epsi) with its significance (sig-epsi), apparent G-band magnitude, as well as the used Apsis-Priam G-band extinction estimate A_G are listed. In the case that the G-band extinction was taken from the StarHorse catalog this is indicated with the SHC flag, or with the ✠ flag if the G-band extinction was derived from V-band extinction measurements, either listed in the VizieR database or from the literature. In this table the exoplanet hosts are indicated with *, and known spectroscopic binary stars among them with (SB).

Table 3 lists for each detected companion its angular separation (ρ) and position angle (PA) to the associated exoplanet host, which were determined with the Gaia DR2 astrometry of the objects for the (Gaia reference) epoch 2015.5. The relative astrometry of the companions exhibits an uncertainty on average of 0.3 mas in angular separation, and 0.002° in position angle, respectively. In the following columns of Tab. 3 we list the parallax difference ($\Delta\pi$) with its significance (in brackets calculated by taking into account also the Gaia astrometric excess noise³) between the exoplanet hosts and their detected companions, their differential proper motion μ_{rel} with its significance, and the cpm-index of all systems. The precise Gaia DR2 astrometry proves the equidistance ($\text{sig-}\Delta\pi < 2.3 \sigma$, average value of 0.5σ) and common proper motion ($\text{cpm-index} > 6$, average $\text{cpm-index} = 118$) of the exoplanet hosts and their companions. If these companions are not listed yet as companion(-candidates) in the Washington Double Star Catalog (WDS from hereon, Mason et al., 2001) this is indicated with the ★ flag in last column of Tab. 3. In the case that the companion is not listed in the WDS but was reported in literature before, additional information is given in the notes of this table.

In Tab. 4 beside the equatorial coordinates (α , δ both for epoch 2015.5) of all detected companions, their derived absolute G-band magnitude M_G , projected separation sep to the associated exoplanet host (relative uncertainty about 1 %, on average), mass, and effective temperature T_{eff} are summarized. The flags listed in the last column of this table are defined as follows:

- PRI: An Apsis-Priam temperature estimate is available for the detected companion, which could be compared with the effective temperature of the companion, derived from its absolute G-band photometry using the Baraffe et al. (2015) models.

³ The astrometric excess noise is conservatively considered here as additional parallax uncertainty of the source.

- 2MA: The companion is listed in the 2MASS Point Source catalogue.
- BPRP: The $G_{BP} - G_{RP}$ color of the exoplanet host and of the detected companion is listed in the Gaia DR2, hence a color comparison was feasible.
- EXT: Because of its brightness the companion exceeds the magnitude range of the Baraffe et al. (2015) evolutionary models. Therefore, the properties of the companion were estimated via extrapolation from the two brightest sources of the used model isochrone.
- WD: The detected companion is a white dwarf.
- BD: The detected companion is a brown dwarf.

Finally, in Tab. 5 we summarize all those detected companions, whose differential proper motion μ_{rel} significantly exceeds their expected escape velocity μ_{rel} . Companions, which are already known to be members of hierarchical triple star systems, are indicated with the flag *** in the last column of this table.

Among all 289 targets, whose multiplicity was investigated in the study, whose results are presented in this paper, 41 binary and 5 hierarchical triple star systems with exoplanets were identified. This yields a multiplicity rate of the targets of $16 \pm 2\%$, very well consistent with the multiplicity rate of exoplanet host stars of $15 \pm 1\%$, reported before by Mugrauer (2019). This is as expected, as the sensitivities of the two surveys should agree well with each other, as the brightness and mass of their targets match, and the distance of the targets from this survey is on average about 40 % smaller than that of the targets from Mugrauer (2019), resulting in a reduction in the distance modulus of only about 1 mag. In total, 61 companions (48 stars and 13 brown dwarfs) could be detected in the Gaia DR2 around the targets. The detected substellar companions are all listed as exoplanets in the EPE. The cumulative distribution functions of the derived properties (projected separation, mass and effective temperature) of these companions, are illustrated in Fig. 3, 4, and 5. The separation-mass diagram of the companions is shown in Fig. 6. As described above, the accurate Gaia DR2 astrometry proves the equidistance and common proper motion of all detected companions with the associated exoplanet hosts, and for the majority of these companions their differential proper motion to the exoplanet hosts is slower than their estimated escape velocity, facts that are expected for gravitationally bound systems. In contrast, the differential proper motion of the companions, which are listed in Tab. 5, exceeds their estimated escape velocity, possibly indicating a higher degree of multiplicity.⁴ Indeed, one of these companions (51 Eri BC) is already known to be a close binary itself. The remaining 2 companions and their primaries are promising targets for follow-up observations to check their multiplicity status e.g. with high contrast AO imaging observations.

All detected companions exhibit projected separations to the associated exoplanet hosts in the range between 52 and 9555 au (average separation of about 2310 au). The highest companion frequency is found at projected separations between about 240 and 400 au and half of all companions are located at projected separations below about 1240 au. The closest detected companion is K2-288 A, which is separated from the exoplanet host stars K2-288 B by 52 au, and it is the only companion identified in this study within a projected separation of 100 au. The masses of the companions range between 0.016 and $1.66 M_{\odot}$ (average mass of $0.36 M_{\odot}$) and companions are found most frequently in the substellar mass regime between 0.016 up to $0.033 M_{\odot}$, while more massive companions are detected at a lower but constant frequency up to about $0.7 M_{\odot}$, and only about 10 % of all the detected companions exhibit masses larger than $0.7 M_{\odot}$. The companions exhibit effective temperatures in the range between about 1850 and 6350 K (average

⁴ Additional close companions either of the exoplanet hosts or of the companions force these objects on close orbits with high orbital velocities around a common barycenter that could induce the observed high differential velocities.

temperature of about 3400 K), which corresponds to spectral types of L3 to F6 (M3, on average), according to the $T_{\text{eff}} - SpT$ relation⁵ from (Pecaut and Mamajek, 2013).

In general the effective temperature of the detected companions, determined with their derived absolute G-band magnitude, using the evolutionary Baraffe et al. (2015) models, agree well with their Gaia DR2 Apsis-Priam temperature estimate (if available) with a characteristic deviation of about ± 350 K, consistent with the typical uncertainty of the different temperature estimates, which is in the order of about 330 K. Only in the case of HIP 38594 B the temperature estimate, based on the absolute G-band photometry of the companion significantly deviates by more than 2300 K from its Apsis-Priam temperature estimate, which is also about 900 K higher than the one of the associated exoplanet host star HIP 38594 A. Furthermore, the companion appears bluer ($\Delta(G_{BP} - G_{RP}) = -0.669 \pm 0.004$ mag) than its primary although it is about 7 mag fainter in the G-band than the exoplanet host star. The intrinsic faintness and high temperature of HIP 38594 B clearly indicates that this companion is a white dwarf. This conclusion is consistent with the results of Subasavage et al. (2008), who have already classified the companion spectroscopically as a white dwarf, and have denote it as WD 0751-252. For this degenerated companion we adopt here a mass of about $0.6 M_{\odot}$.

In Fig. 7 the G-band magnitude difference of all detected companions to the associated exoplanet hosts is plotted versus their angular separation. For comparison we show as dashed line in this figure the estimate of the Gaia detection limit, reported by Mugrauer (2019) which was further constrained by Mugrauer and Michel (2020). Companions of exoplanet hosts brighter than 12.8 mag are plotted as open circles those of hosts, which are fainter than that magnitude limit, as filled black circles, respectively. A magnitude difference of about 5 mag is reached at an angular separation of about 2 arcsec, consistent with the estimate of the Gaia detection limit, determined by Mugrauer (2019). Only two companions significantly exceed the limit estimate, namely K2-288 A at an angular separation of about 0.8 arcsec with $\Delta G \sim 1.2$ mag and HIP 77900 B, at 22.3 arcsec with $\Delta G \sim 13.5$ mag. While K2-288 A is a companion of a target fainter than $G = 12.8$ mag for which Gaia reaches a higher sensitivity at angular separations slightly below 1 arcsec (up to 3 mag, as described by Mugrauer and Michel, 2020) the detection of HIP 77900 B indicates that the given limit estimate might be too conservative at angular separations beyond about 20 arcsec.

4 SUMMARY AND OUTLOOK

The study, presented here, is a continuation of a survey, which was initiated at the Astrophysical Institute and University Observatory Jena, to investigate the multiplicity status of exoplanet hosts and to characterize the properties of their detected (sub)stellar companions, using accurate Gaia astro- and photometry. In this paper the multiplicity of 289 exoplanet hosts was explored and (sub)stellar companions were detected around 60 targets. The companionship of these objects with the exoplanet hosts could be proven with their accurate Gaia DR2 astrometry (equidistance, common proper motion, and differential proper motion smaller than the expected escape velocity). The mass and effective temperature of all companions were determined with their derived absolute G-band photometry and the Baraffe et al. (2015) evolutionary models of (sub)stellar objects. In total, 61 companions (beside 48 stellar companions, among them the white dwarf HIP 38594 B, also 13 brown dwarfs) were detected in this project, and 14 of these objects are neither listed in the WDS as companion(-candidate)s of the targets nor were described in the literature before. A total of 41 binary and 5 triple star systems with exoplanets, were identified in this study, yielding a multiplicity rate of the targets of about 16 %, which is very well consistent with the multiplicity rate of exoplanet host stars, reported by Mugrauer (2019). Following the standard procedure of our survey, all detected companions

⁵ Online available at: http://www.pas.rochester.edu/~emamajek/EEM_dwarf_UBVIJHK_colors_Teff.txt

and their derived properties will be made available online in the `VizieR` database. The survey, whose latest results are presented here, is an ongoing project as more and more exoplanet hosts are detected by different planet detection methods, whose multiplicity status needs to be investigated. Furthermore, there are sources, listed in the Gaia DR2, within the applied search radius around the targets, which still lack a five parameter astrometric solution. Hence, further companions of the exoplanet hosts, investigated here, should exist, whose companionship can be proven with accurate astrometric measurements, provided by future data releases of the ESA-Gaia mission, e.g. the Gaia EDR3, planed to be published end of 2020.

The results of this survey, which is mainly sensitive for wide companions of exoplanet hosts, combined with those of our currently ongoing large high contrast imaging surveys (sensitive for close companions), carried out with SPHERE/VLT and AstraLux/CAHA (first results are already published e.g. by Ginski et al., 2020) will yield a complete characterization of the multiplicity status of the observed targets. This will eventually allow to draw conclusions on the impact of the stellar multiplicity on the formation process of planets and the evolution of their orbits.

ACKNOWLEDGMENTS

We thank the two anonymous referees for their helpful and constructive comments on the manuscript.

We made use of data from:

(1) the `Simbad` and `VizieR` databases, both operated at CDS in Strasbourg, France.

(2) the European Space Agency (ESA) mission Gaia (<https://www.cosmos.esa.int/gaia>), processed by the Gaia Data Processing and Analysis Consortium (DPAC, <https://www.cosmos.esa.int/web/gaia/dpac/consortium>). Funding for the DPAC has been provided by national institutions, in particular the institutions participating in the Gaia Multilateral Agreement.

(3) the Two Micron All Sky Survey, which is a joint project of the University of Massachusetts and the Infrared Processing and Analysis Center/California Institute of Technology, funded by the National Aeronautics and Space Administration and the National Science Foundation.

REFERENCES

- Aller, K. M., Kraus, A. L., Liu, M. C., Burgett, W. S., Chambers, K. C., Hodapp, K. W., et al. (2013). A Pan-STARRS + UKIDSS Search for Young, Wide Planetary-mass Companions in Upper Scorpius. *ApJ* 773, 63. doi:10.1088/0004-637X/773/1/63
- Anders, F., Khalatyan, A., Chiappini, C., Queiroz, A. B., Santiago, B. X., Jordi, C., et al. (2019). Photo-astrometric distances, extinctions, and astrophysical parameters for Gaia DR2 stars brighter than $G = 18$. *A&A* 628, A94. doi:10.1051/0004-6361/201935765
- Bailer-Jones, C. A. L., Andrae, R., Arcay, B., Astraatmadja, T., Bellas-Velidis, I., Berihuete, A., et al. (2013). The Gaia astrophysical parameters inference system (Apsis). Pre-launch description. *A&A* 559, A74. doi:10.1051/0004-6361/201322344
- Baraffe, I., Homeier, D., Allard, F., and Chabrier, G. (2015). New evolutionary models for pre-main sequence and main sequence low-mass stars down to the hydrogen-burning limit. *A&A* 577, A42. doi:10.1051/0004-6361/201425481
- Basri, G. (2000). Observations of Brown Dwarfs. *ARA&A* 38, 485–519. doi:10.1146/annurev.astro.38.1.485

- Bowler, B. P. and Hillenbrand, L. A. (2015). Near-infrared Spectroscopy of 2M0441+2301 AabBab: A Quadruple System Spanning the Stellar to Planetary Mass Regimes. *ApJL* 811, L30. doi:10.1088/2041-8205/811/2/L30
- Bowler, B. P., Kraus, A. L., Bryan, M. L., Knutson, H. A., Brogi, M., Rizzuto, A. C., et al. (2017). The Young Substellar Companion ROXs 12 B: Near-infrared Spectrum, System Architecture, and Spin-Orbit Misalignment. *AJ* 154, 165. doi:10.3847/1538-3881/aa88bd
- Bowler, B. P., Liu, M. C., Shkolnik, E. L., Dupuy, T. J., Cieza, L. A., Kraus, A. L., et al. (2012). Planets around Low-mass Stars (PALMS). I. A Substellar Companion to the Young M Dwarf 1RXS J235133.3+312720. *ApJ* 753, 142. doi:10.1088/0004-637X/753/2/142
- Burgasser, A. J., Looper, D. L., and Kirkpatrick, J. D. (2017). A Candidate Wide Brown Dwarf Binary in the Argus Association: 2MASS J14504216-7841413 and 2MASS J14504113-7841383. *RNAAS* 1, 42. doi:10.3847/2515-5172/aa9ff0
- Dickson-Vandervelde, D. A., Wilson, E. C., and Kastner, J. H. (2020). Identification of the Youngest Known Substellar Object within ~ 100 pc. *RNAAS* 4, 25. doi:10.3847/2515-5172/ab7344
- Dorval, P., Talens, G. J. J., Otten, G. P. P. L., Brahm, R., Jordán, A., Torres, P., et al. (2020). MASCARA-4 b/bRing-1 b: A retrograde hot Jupiter around a bright A-type star. *A&A* 635, A60. doi:10.1051/0004-6361/201935611
- Duchêne, G. and Kraus, A. (2013). Stellar Multiplicity. *ARA&A* 51, 269–310. doi:10.1146/annurev-astro-081710-102602
- Feinstein, A. D., Schlieder, J. E., Livingston, J. H., Ciardi, D. R., Howard, A. W., Arnold, L., et al. (2019). K2-288Bb: A Small Temperate Planet in a Low-mass Binary System Discovered by Citizen Scientists. *AJ* 157, 40. doi:10.3847/1538-3881/aafa70
- Gaia Collaboration, Brown, A. G. A., Vallenari, A., Prusti, T., de Bruijne, J. H. J., Babusiaux, C., et al. (2018). Gaia Data Release 2. Summary of the contents and survey properties. *A&A* 616, A1. doi:10.1051/0004-6361/201833051
- Geißler, K., Metchev, S. A., Pham, A., Larkin, J. E., McElwain, M., and Hillenbrand, L. A. (2012). A Substellar Common Proper-motion Companion to the Pleiad H II 1348. *ApJ* 746, 44. doi:10.1088/0004-637X/746/1/44
- Ginski, C., Mugrauer, M., Adam, C., Vogt, N., and van Holstein, R. (2020). How many suns are in the sky? A SPHERE multiplicity survey of exoplanet host stars I – Four new close stellar companions including a white dwarf. *arXiv e-prints*, arXiv:2009.10363
- Hartman, J. D., Jordán, A., Bayliss, D., Bakos, G. Á., Bento, J., Bhatti, W., et al. (2020). HATS-47b, HATS-48Ab, HATS-49b, and HATS-72b: Four Warm Giant Planets Transiting K Dwarfs. *AJ* 159, 173. doi:10.3847/1538-3881/ab7821
- Hinkley, S., Kraus, A. L., Ireland, M. J., Cheetham, A., Carpenter, J. M., Tuthill, P., et al. (2015). Discovery of Seven Companions to Intermediate-mass Stars with Extreme Mass Ratios in the Scorpius-Centaurus Association. *ApJL* 806, L9. doi:10.1088/2041-8205/806/1/L9
- Hjorth, M., Justesen, A. B., Hirano, T., Albrecht, S., Gandolfi, D., Dai, F., et al. (2019). K2-290: a warm Jupiter and a mini-Neptune in a triple-star system. *MNRAS* 484, 3522–3536. doi:10.1093/mnras/stz139
- Itoh, Y., Hayashi, M., Tamura, M., Tsuji, T., Oasa, Y., Fukagawa, M., et al. (2005). A Young Brown Dwarf Companion to DH Tauri. *ApJ* 620, 984–993. doi:10.1086/427086
- Jackman, J. A. G., Wheatley, P. J., Bayliss, D., Gill, S., Hodgkin, S. T., Burleigh, M. R., et al. (2019). NGTS-7Ab: an ultrashort-period brown dwarf transiting a tidally locked and active M dwarf. *MNRAS* 489, 5146–5164. doi:10.1093/mnras/stz2496
- Janson, M., Asensio-Torres, R., André, D., Bonnefoy, M., Delorme, P., Reffert, S., et al. (2019). The

- B-Star Exoplanet Abundance Study: a co-moving 16-25 M_{Jup} companion to the young binary system HIP 79098. *A&A* 626, A99. doi:10.1051/0004-6361/201935687
- Johns, D., Reed, P. A., Rodriguez, J. E., Pepper, J., Stassun, K. G., Penev, K., et al. (2019). KELT-23Ab: A Hot Jupiter Transiting a Near-solar Twin Close to the TESS and JWST Continuous Viewing Zones. *AJ* 158, 78. doi:10.3847/1538-3881/ab24c7
- Kraus, A. L., Ireland, M. J., Cieza, L. A., Hinkley, S., Dupuy, T. J., Bowler, B. P., et al. (2014). Three Wide Planetary-mass Companions to FW Tau, ROXs 12, and ROXs 42B. *ApJ* 781, 20. doi:10.1088/0004-637X/781/1/20
- Mason, B. D., Wycoff, G. L., Hartkopf, W. I., et al. (2001). The 2001 US Naval Observatory Double Star CD-ROM. I. The Washington Double Star Catalog. *AJ* 122, 3466
- McCormac, J., Gillen, E., Jackman, J. A. G., Brown, D. J. A., Bayliss, D., Wheatley, P. J., et al. (2020). NGTS-10b: the shortest period hot Jupiter yet discovered. *MNRAS* 493, 126–140. doi:10.1093/mnras/staa115
- Mugrauer, M. (2019). Search for stellar companions of exoplanet host stars by exploring the second ESA-Gaia data release. *MNRAS* 490, 5088–5102. doi:10.1093/mnras/stz2673
- Mugrauer, M. and Ginski, C. (2015). High-contrast imaging search for stellar and substellar companions of exoplanet host stars. *MNRAS* 450, 3127–3136. doi:10.1093/mnras/stv771
- Mugrauer, M., Ginski, C., and Seeliger, M. (2014). New wide stellar companions of exoplanet host stars. *MNRAS* 439, 1063–1070. doi:10.1093/mnras/stu044
- Mugrauer, M. and Michel, K. U. (2020). Gaia Search for stellar Companions of TESS Objects of Interest. *arXiv e-prints*, arXiv:2009.12234
- Neuhäuser, R., Guenther, E. W., Wuchterl, G., Mugrauer, M., Bedalov, A., and Hauschildt, P. H. (2005). Evidence for a co-moving sub-stellar companion of GQ Lup. *A&A* 435, L13–L16. doi:10.1051/0004-6361:200500104
- Nielsen, E. L., Liu, M. C., Wahhaj, Z., Biller, B. A., Hayward, T. L., Boss, A., et al. (2012). The Gemini NICI Planet-Finding Campaign: Discovery of a Multiple System Orbiting the Young A Star HD 1160. *ApJ* 750, 53. doi:10.1088/0004-637X/750/1/53
- Nielsen, L. D., Bouchy, F., Turner, O. D., Anderson, D. R., Barkaoui, K., Benkhaldoun, Z., et al. (2019). WASP-169, WASP-171, WASP-175, and WASP-182: three hot Jupiters and one bloated sub-Saturn mass planet discovered by WASP-South. *MNRAS* 489, 2478–2487. doi:10.1093/mnras/stz2351
- Ochsenbein, F., Bauer, P., and Marcout, J. (2000). The VizieR database of astronomical catalogues. *A&AS* 143, 23–32. doi:10.1051/aas:2000169
- Pecaut, M. J. and Mamajek, E. E. (2013). Intrinsic Colors, Temperatures, and Bolometric Corrections of Pre-main-sequence Stars. *ApJS* 208, 9. doi:10.1088/0067-0049/208/1/9
- Ricker, G. R., Winn, J. N., Vanderspek, R., Latham, D. W., Bakos, G. Á., Bean, J. L., et al. (2015). Transiting Exoplanet Survey Satellite (TESS). *JATIS* 1, 014003. doi:10.1117/1.JATIS.1.1.014003
- Rodriguez, J. E., Eastman, J. D., Zhou, G., Quinn, S. N., Beatty, T. G., Penev, K., et al. (2019). KELT-24b: A 5 M_J Planet on a 5.6 day Well-aligned Orbit around the Young V = 8.3 F-star HD 93148. *AJ* 158, 197. doi:10.3847/1538-3881/ab4136
- Schneider, J., Dedieu, C., Le Sidaner, P., Savalle, R., and Zolotukhin, I. (2011). Defining and cataloging exoplanets: the exoplanet.eu database. *A&A* 532, A79. doi:10.1051/0004-6361/201116713
- Skrutskie, M. F., Cutri, R. M., Stiening, R., Weinberg, M. D., Schneider, S., Carpenter, J. M., et al. (2006). The Two Micron All Sky Survey (2MASS). *AJ* 131, 1163–1183. doi:10.1086/498708
- Smart, R. L. and Nicastrò, L. (2014). The initial Gaia source list. *A&A* 570, A87. doi:10.1051/0004-6361/201424241

- Subasavage, J. P., Henry, T. J., Bergeron, P., Dufour, P., and Hambly, N. C. (2008). The Solar Neighborhood. Xx. Discovery and Characterization of 21 New Nearby White Dwarf Systems. *AJ* 136, 899–908. doi:10.1088/0004-6256/136/3/899
- Triaud, A. H. M. J., Burgasser, A. J., Burdanov, A., Kunovac Hodžić, V., Alonso, R., Bardalez Gagliuffi, D., et al. (2020). An eclipsing substellar binary in a young triple system discovered by SPECULOOS. *NatAs* 4, 650–657. doi:10.1038/s41550-020-1018-2
- van Leeuwen, F. (2007). Validation of the new Hipparcos reduction. *A&A* 474, 653–664. doi:10.1051/0004-6361:20078357
- Vanderburg, A., Huang, C. X., Rodriguez, J. E., Becker, J. C., Ricker, G. R., Vanderspek, R. K., et al. (2019). TESS Spots a Compact System of Super-Earths around the Naked-eye Star HR 858. *ApJL* 881, L19. doi:10.3847/2041-8213/ab322d

5 TABLES

Table 1. The properties of all targets of this study. The corresponding histograms are shown in Fig. 1.

	Distance [pc]	μ [mas/yr]	G [mag]	age [Gyr]	mass [M_{\odot}]
min	1.8	1.7	3.7	0.001	0.016
max	586	10394	20.8	14.9	20
ave	137	270	10.8	3.5	1.1
med	94	65	10.7	2.1	1.0

Table 2. Gaia astro- and photometry of all exoplanet hosts and their companions, detected in this study.

Name	π [mas]	$\mu_{\alpha \cos(\delta)}$ [mas/yr]	μ_{δ} [mas/yr]	epsi [mas]	sig-epsi	G [mag]	A_G [mag]
HD 1160 A*	7.9417 \pm 0.0764	20.089 \pm 0.138	-14.575 \pm 0.099	0.121	6.0	7.1074 \pm 0.0003	0.1347 ^{+0.1300} _{-0.0968}
HD 1160 C	6.9946 \pm 0.2739	20.605 \pm 0.333	-16.215 \pm 0.311	0.739	37	15.3505 \pm 0.0207	
Gliese 49 A*	101.4650 \pm 0.0335	731.135 \pm 0.041	90.690 \pm 0.048	—	—	8.6628 \pm 0.0007	0.6030 ^{+0.2220} _{-0.4095}
Gliese 49 B	101.6371 \pm 0.0806	730.740 \pm 0.163	86.352 \pm 0.225	0.190	13	11.9238 \pm 0.0033	
HD 8326 A*	32.5591 \pm 0.0466	-58.470 \pm 0.120	-224.887 \pm 0.064	—	—	8.4749 \pm 0.0004	
HD 8326 B	32.4362 \pm 0.0589	-57.577 \pm 0.156	-224.122 \pm 0.088	0.347	27	14.2066 \pm 0.0006	0.2940 ^{+0.2446} _{-0.0438}
HD 13167 A*	6.6859 \pm 0.0485	43.770 \pm 0.077	-38.126 \pm 0.079	—	—	8.1600 \pm 0.0003	
HD 13167 B	6.7931 \pm 0.1254	44.134 \pm 0.215	-39.358 \pm 0.212	0.444	3.3	17.4513 \pm 0.0022	0.2431 ^{+0.0597} _{-0.0648} SHC
HR 858 A*	31.2565 \pm 0.0700	123.229 \pm 0.070	105.788 \pm 0.151	0.086	3.9	6.2480 \pm 0.0003	0.1320 ^{+0.1061} _{-0.0911}
HR 858 B	32.3014 \pm 0.1670	137.125 \pm 0.213	105.865 \pm 0.302	0.835	63	16.0464 \pm 0.0031	
HD 18015 A*	8.0490 \pm 0.0517	63.053 \pm 0.089	-4.359 \pm 0.082	—	—	7.7219 \pm 0.0005	
HD 18015 B	7.9413 \pm 0.0415	64.638 \pm 0.071	-4.668 \pm 0.066	—	—	12.2361 \pm 0.0008	0.1440 ^{+0.0361} _{-0.0325}
K2-288 B*	15.2166 \pm 0.2007	185.476 \pm 0.708	-74.070 \pm 0.618	0.766	70	14.5451 \pm 0.0017	
K2-288 A	14.2879 \pm 0.0807	187.057 \pm 0.151	-69.591 \pm 0.116	0.418	41	13.3090 \pm 0.0009	0.5668 ^{+0.0884} _{-0.0824} SHC
HD 23472 A*	25.5897 \pm 0.0261	-102.571 \pm 0.050	-43.917 \pm 0.059	—	—	9.3848 \pm 0.0002	0.0783 ^{+0.1742} _{-0.0703}
HD 23472 B	25.5060 \pm 0.0732	-103.019 \pm 0.154	-42.771 \pm 0.169	0.490	16.1	15.8312 \pm 0.0014	
HD 24085 B*	18.1859 \pm 0.0245	-9.249 \pm 0.048	-97.358 \pm 0.050	—	—	7.4250 \pm 0.0002	
HD 24085 A	18.1430 \pm 0.0226	-10.234 \pm 0.043	-97.151 \pm 0.049	—	—	7.2719 \pm 0.0002	0.6682 ^{+0.5911} _{-0.3903}
HII 1348 A* (SB)	6.9890 \pm 0.0490	21.401 \pm 0.120	-45.705 \pm 0.060	—	—	12.2439 \pm 0.0012	
HII 1348 C	6.6456 \pm 0.1763	20.250 \pm 0.337	-45.292 \pm 0.235	0.429	4.1	17.0303 \pm 0.0017	1.1810 ^{+0.3091} _{-0.3321}
HII 1348 D	7.8946 \pm 1.7831	23.361 \pm 4.630	-42.219 \pm 2.330	2.369	0.9	20.7790 \pm 0.0151	0.6550 ^{+0.3718} _{-0.4581}
HATS-57 A*	3.5495 \pm 0.0392	-12.664 \pm 0.046	-14.115 \pm 0.040	—	—	12.1816 \pm 0.0007	0.0548 ^{+0.1726} _{-0.0423}
HATS-57 B	3.4904 \pm 0.1265	-12.064 \pm 0.174	-14.764 \pm 0.142	—	—	17.5558 \pm 0.0012	
FU Tau A*	7.5981 \pm 0.1497	6.895 \pm 0.376	-21.026 \pm 0.202	0.732	83	15.2412 \pm 0.0024	2.2620 ^{+0.2597} _{-0.4841}
FU Tau B	7.4909 \pm 1.2887	12.450 \pm 4.056	-21.761 \pm 1.903	3.516	4.6	20.4799 \pm 0.0074	
DH Tau A*	7.3880 \pm 0.0693	7.065 \pm 0.117	-20.699 \pm 0.079	—	—	12.4961 \pm 0.0090	
DH Tau C	7.4011 \pm 0.0520	6.899 \pm 0.113	-21.207 \pm 0.074	—	—	11.9692 \pm 0.0013	2.6683 ^{+0.3698} _{-0.1714}
51 Eri A*	33.5770 \pm 0.1354	44.352 \pm 0.227	-63.833 \pm 0.178	0.562	190	5.1224 \pm 0.0017	0.1740 ^{+0.2663} _{-0.1123}
51 Eri B (SB)	37.9633 \pm 0.3662	59.587 \pm 0.717	-52.419 \pm 0.618	1.958	2030	9.7247 \pm 0.0011	
2M0441+23 C*	8.3040 \pm 0.3778	8.955 \pm 0.931	-21.431 \pm 0.456	1.350	5.7	18.9668 \pm 0.0068	
2M0441+23 AB	8.0161 \pm 0.0832	8.300 \pm 0.189	-21.553 \pm 0.103	0.529	79	13.8267 \pm 0.0011	1.0577 ^{+0.9503} _{-0.4138}

Table 2. continued

Name	π [mas]	$\mu_{\alpha}\cos(\delta)$ [mas/yr]	μ_{δ} [mas/yr]	$epsi$ [mas]	$sig-epsi$	G [mag]	A_G [mag]
NGTS-6 A*	3.2151 \pm 0.0148	-9.339 \pm 0.025	-21.9950 \pm 0.026	—	—	13.8175 \pm 0.0006	—
NGTS-6 B	3.2231 \pm 0.0653	-9.301 \pm 0.107	-22.1300 \pm 0.114	0.203	1.3	17.0603 \pm 0.0009	0.3627 ^{+0.1024} _{-0.1403}
AB Dor AC*	65.3199 \pm 0.1440	29.150 \pm 0.251	164.4210 \pm 0.299	0.850	317	6.6738 \pm 0.0018	—
AB Dor BD	67.0283 \pm 0.0901	66.366 \pm 0.155	125.8990 \pm 0.189	0.522	111	11.3560 \pm 0.0012	1.3528 ^{+0.5192} _{-0.4435}
HD 39855 A*	42.9636 \pm 0.0346	92.854 \pm 0.046	-24.4660 \pm 0.063	—	—	7.3211 \pm 0.0002	—
HD 39855 B	42.9612 \pm 0.0369	96.166 \pm 0.055	-11.8960 \pm 0.065	—	—	10.0503 \pm 0.0006	0.1920 ^{+0.2268} _{-0.1257}
NGTS-10 A*	3.0798 \pm 0.2610	-2.323 \pm 0.343	10.5270 \pm 0.395	2.152	1100	14.2604 \pm 0.0034	—
NGTS-10 B	0.2965 \pm 0.0802	-1.120 \pm 0.219	9.6710 \pm 0.161	0.064	0.3	15.5926 \pm 0.0014	0.7679 ^{+1.1986} _{-0.5770} SHC
L2 Pup A*	15.61 \pm 0.99	106.31 \pm 0.96	324.99 \pm 1.08	—	—	9.8208 \pm 0.2812	HIP
L2 Pup B	16.4131 \pm 0.0574	105.895 \pm 0.097	327.272 \pm 0.099	0.368	12	15.7099 \pm 0.0009	0.2940 ^{+0.3029} _{-0.0934}
HIP 38594 A*	56.1868 \pm 0.0297	-300.905 \pm 0.044	200.923 \pm 0.045	—	—	9.0853 \pm 0.0003	—
HIP 38594 B	56.1234 \pm 0.0799	-297.867 \pm 0.126	206.598 \pm 0.257	—	—	16.0444 \pm 0.0005	0.3670 ^{+0.7758} _{-0.2630}
WASP-180 A*	3.9093 \pm 0.0517	-14.052 \pm 0.091	-3.169 \pm 0.055	—	—	10.9134 \pm 0.0007	—
WASP-180 B	3.8618 \pm 0.0734	-12.705 \pm 0.172	-2.710 \pm 0.103	—	—	11.7712 \pm 0.0008	0.0930 ^{+0.1560} _{-0.0534}
HD 79211 B*	157.8851 \pm 0.0414	-1573.120 \pm 0.061	-660.121 \pm 0.058	—	—	7.0477 \pm 0.0004	—
HD 79211 A	157.8796 \pm 0.0366	-1546.100 \pm 0.059	-569.127 \pm 0.060	—	—	6.9689 \pm 0.0005	0.3757 ^{+0.3264} _{-0.2078}
HD 85628 A*	5.8297 \pm 0.0318	6.051 \pm 0.055	-15.398 \pm 0.051	—	—	8.1740 \pm 0.0004	0.5012 ^{+0.1438} _{-0.2262}
HD 85628 B	5.9508 \pm 0.0366	5.856 \pm 0.066	-13.252 \pm 0.060	0.296	18	14.0490 \pm 0.0047	—
TOI 717 A*	28.7709 \pm 0.0783	-26.092 \pm 0.176	62.064 \pm 0.260	0.045	0.5	12.6410 \pm 0.0005	0.3110 ^{+0.1274} _{-0.0211}
TOI 717 B	28.7588 \pm 0.0824	-23.995 \pm 0.177	62.081 \pm 0.273	0.060	1.0	12.7386 \pm 0.0008	—
G 196-3 A*	45.8611 \pm 0.0388	-141.177 \pm 0.055	-202.394 \pm 0.053	0.000	0.5	10.6123 \pm 0.0005	1.0645 ^{+0.4919} _{-0.4836}
G 196-3 B	44.3549 \pm 0.8128	-137.820 \pm 0.928	-208.523 \pm 1.671	2.210	3.3	20.1697 \pm 0.0085	—
LTT 3780 A*	45.4644 \pm 0.0827	-341.409 \pm 0.114	-247.870 \pm 0.105	0.137	6.6	11.8465 \pm 0.0005	0.5015 ^{+0.2595} _{-0.3436}
LTT 3780 B	45.2879 \pm 0.1081	-341.379 \pm 0.149	-248.419 \pm 0.135	0.414	23	14.4855 \pm 0.0008	—
MASCARA-3 A*	10.3320 \pm 0.0333	-56.184 \pm 0.053	-34.808 \pm 0.064	—	—	8.2375 \pm 0.0004	0.2400 ^{+0.2740} _{-0.1150}
MASCARA-3 B	11.0260 \pm 0.1268	-50.757 \pm 0.325	-37.811 \pm 0.200	0.799	160	13.0002 \pm 0.0109	—
2M J1101-7732 A*	5.4081 \pm 0.1877	-22.653 \pm 0.435	2.062 \pm 0.397	1.271	12	18.3299 \pm 0.0023	—
2M J1101-7732 B	5.4333 \pm 0.3368	-23.668 \pm 0.748	1.931 \pm 0.723	1.836	6.1	19.4040 \pm 0.0047	0.5900 ^{+0.1200} _{-0.1200} ✠
WASP-175 A*	1.8260 \pm 0.0399	-24.306 \pm 0.057	6.033 \pm 0.057	—	—	12.7065 \pm 0.0002	—
WASP-175 B	1.7947 \pm 0.0308	-24.064 \pm 0.045	6.185 \pm 0.045	—	—	14.2462 \pm 0.0003	0.0965 ^{+0.0966} _{-0.0876}

Table 2. continued

Name	π [mas]	$\mu_{\alpha} \cos(\delta)$ [mas/yr]	μ_{δ} [mas/yr]	ϵ_{psi} [mas]	sig- ϵ_{psi}	G [mag]	A_G [mag]
CHXR 73 A*	5.2343 \pm 0.1759	-22.193 \pm 0.233	0.215 \pm 0.206	0.815	12	17.2934 \pm 0.0014	3.4650 $^{+1.0250}_{-1.0250}$ ✠
CHXR 73 C	5.2502 \pm 0.2218	-22.937 \pm 0.433	-1.261 \pm 0.347	1.241	14	17.9098 \pm 0.0021	
GJ 414 A*	84.0803 \pm 0.0471	591.622 \pm 0.081	-197.247 \pm 0.091	—	—	7.7281 \pm 0.0007	
GJ 414 B	84.1971 \pm 0.0579	604.831 \pm 0.081	-206.442 \pm 0.075	—	—	9.0471 \pm 0.0011	0.6100 $^{+0.5656}_{-0.3221}$
HD 97334 A*	44.1428 \pm 0.0383	-249.387 \pm 0.090	-151.590 \pm 0.071	—	—	6.2410 \pm 0.0006	0.0555 $^{+0.1848}_{-0.0415}$
HD 97334 BC	42.8724 \pm 1.1025	-236.349 \pm 2.133	-152.068 \pm 2.109	5.342	15	19.9859 \pm 0.0135	
HD 233832 A*	16.9952 \pm 0.0752	-473.960 \pm 0.075	124.167 \pm 0.087	—	—	9.9456 \pm 0.0005	
HD 233832 B	17.0667 \pm 0.0532	-478.645 \pm 0.048	119.122 \pm 0.088	—	—	12.7187 \pm 0.0004	0.2288 $^{+0.2054}_{-0.1079}$
2MJ1155-7919 A*	9.8862 \pm 0.0585	-41.179 \pm 0.127	-4.336 \pm 0.086	0.490	35	14.8180 \pm 0.0017	0.4158 $^{+0.0616}_{-0.0052}$ ✠
2MJ1155-7919 B	9.8211 \pm 0.5264	-39.738 \pm 1.216	-4.656 \pm 0.687	1.387	1.4	19.9246 \pm 0.0079	
NGTS-5 A*	3.2310 \pm 0.0272	13.650 \pm 0.041	-4.688 \pm 0.042	—	—	13.5260 \pm 0.0004	0.1970 $^{+0.1050}_{-0.1174}$
NGTS-5 B	2.9428 \pm 0.1254	13.938 \pm 0.209	-4.331 \pm 0.180	0.422	3.0	17.3160 \pm 0.0016	
2MJ1450-7841 A*	10.9480 \pm 0.5046	-37.597 \pm 0.881	-23.654 \pm 0.895	2.345	5.0	19.6858 \pm 0.0060	0.5000 $^{+0.5000}_{-0.5000}$ ✠
2MJ1450-7841 B	8.6592 \pm 0.9023	-34.984 \pm 2.047	-22.162 \pm 1.764	2.067	1.1	20.6501 \pm 0.0097	
WASP-189 A*	9.9990 \pm 0.0747	-50.564 \pm 0.109	-23.788 \pm 0.115	0.082	2.2	6.5537 \pm 0.0004	0.2652 $^{+0.1599}_{-0.2306}$ SHC
WASP-189 B	10.7202 \pm 0.1648	-50.594 \pm 0.165	-24.037 \pm 0.178	0.475	25	14.3874 \pm 0.0024	
HIP 73990 A*	9.0326 \pm 0.0648	-27.432 \pm 0.106	-29.028 \pm 0.089	—	—	8.0678 \pm 0.0009	
HIP 73990 D	8.9507 \pm 0.0899	-27.728 \pm 0.159	-29.245 \pm 0.135	0.457	28	14.6580 \pm 0.0007	1.1073 $^{+0.6427}_{-0.4489}$
TOI 905 A*	6.2745 \pm 0.0285	-25.839 \pm 0.033	-41.150 \pm 0.051	—	—	11.0813 \pm 0.0004	0.2703 $^{+0.1330}_{-0.1606}$ SHC
TOI 905 B	7.8542 \pm 0.5489	-18.290 \pm 0.763	-39.819 \pm 0.788	1.423	25	17.2149 \pm 0.0375	
2M 1510 A*	27.2203 \pm 0.2665	-118.747 \pm 0.492	-46.865 \pm 0.420	1.112	18	17.4870 \pm 0.0018	0.9266 $^{+0.1360}_{-0.0121}$ SHC
2M 1510 B	27.6869 \pm 0.4939	-117.448 \pm 0.893	-45.713 \pm 0.746	1.710	7.8	18.8855 \pm 0.0035	
β Cir A*	35.1736 \pm 0.4253	-96.742 \pm 0.491	-136.541 \pm 0.621	1.852	1770	3.9732 \pm 0.0026	0.2560 $^{+0.2260}_{-0.1598}$
β Cir B	34.7836 \pm 0.6840	-92.763 \pm 0.829	-138.156 \pm 1.469	2.701	15	19.4335 \pm 0.0051	
KELT-23 A*	7.8912 \pm 0.0219	0.434 \pm 0.039	-12.217 \pm 0.041	—	—	10.1820 \pm 0.0004	0.0680 $^{+0.0996}_{-0.0505}$
KELT-23 B	7.8949 \pm 0.0529	1.567 \pm 0.093	-11.903 \pm 0.107	0.284	6.8	15.5209 \pm 0.0014	
K2-290 A*B	3.6365 \pm 0.0503	27.225 \pm 0.099	-16.893 \pm 0.066	—	—	10.8204 \pm 0.0004	0.8900 $^{+0.2570}_{-0.2655}$
K2-290 C	4.0531 \pm 0.2711	27.465 \pm 0.593	-16.484 \pm 0.370	0.556	1.2	18.5920 \pm 0.0027	
GQ Lup A*	6.5868 \pm 0.0473	-14.257 \pm 0.097	-23.596 \pm 0.066	0.110	5.7	11.2608 \pm 0.0089	2.7645 $^{+0.3426}_{-0.4140}$
GQ Lup C	5.4925 \pm 0.4597	-14.807 \pm 0.972	-21.947 \pm 0.653	2.960	59	18.3740 \pm 0.0037	

Table 2. continued

Name	π [mas]	$\mu_{\alpha\cos(\delta)}$ [mas/yr]	μ_{δ} [mas/yr]	ϵ_{psi} [mas]	$\text{sig-}\epsilon_{\text{psi}}$	G [mag]	A_G [mag]
HIP 77900 A*	6.6037 \pm 0.1196	-13.357 \pm 0.187	-25.272 \pm 0.110	0.212	21	6.1129 \pm 0.0006	0.1852 $^{+0.1535}_{-0.0360}$
HIP 77900 B	5.2279 \pm 0.9696	-13.908 \pm 1.517	-23.265 \pm 1.097	2.007	4.3	19.5660 \pm 0.0057	
USco 1602-2401 A*	6.9484 \pm 0.0661	-11.850 \pm 0.119	-24.032 \pm 0.051	—	—	11.8656 \pm 0.0026	1.8885 $^{+0.1123}_{-0.1186}$ SHC
USco 1602-2401 B	6.3381 \pm 0.2030	-12.699 \pm 0.325	-23.872 \pm 0.187	0.829	40	16.3640 \pm 0.0010	
HIP 79098 A (SB)*	6.8337 \pm 0.1176	-9.823 \pm 0.210	-28.119 \pm 0.163	0.289	35	5.8264 \pm 0.0006	0.4640 $^{+0.1440}_{-0.2381}$
HIP 79098 C	7.1870 \pm 0.1476	-10.979 \pm 0.271	-26.128 \pm 0.189	0.666	27	16.1091 \pm 0.0012	
USco 1610-1913 A*	7.4960 \pm 0.0718	-9.342 \pm 0.206	-23.591 \pm 0.111	0.168	12	12.6962 \pm 0.0049	0.3850 $^{+0.3850}_{-0.3850}$ ✖
USco 1610-1913 B	6.9600 \pm 0.3719	-7.043 \pm 1.112	-24.982 \pm 0.576	1.301	7.0	18.7225 \pm 0.0029	
USco 1612-1800 A*	6.3156 \pm 0.0747	-7.418 \pm 0.161	-21.148 \pm 0.112	0.427	31	14.5532 \pm 0.0007	0.3850 $^{+0.3850}_{-0.3850}$ ✖
USco 1612-1800 B	6.0413 \pm 0.3224	-7.002 \pm 0.698	-19.738 \pm 0.512	1.112	4.0	18.8810 \pm 0.0032	
ROXs 12 A*	7.2894 \pm 0.0417	-7.185 \pm 0.090	-24.851 \pm 0.059	0.158	6.9	13.2655 \pm 0.0013	1.8000 $^{+1.0000}_{-1.0000}$ ✖
ROXs 12 C	7.2328 \pm 0.0738	-6.577 \pm 0.151	-25.106 \pm 0.099	0.354	20	14.7659 \pm 0.0113	
HATS-48 A*	3.7648 \pm 0.0237	3.125 \pm 0.031	6.146 \pm 0.029	—	—	13.8951 \pm 0.0002	0.5090 $^{+0.1876}_{-0.3705}$
HATS-48 B	3.6354 \pm 0.4432	2.951 \pm 0.469	5.201 \pm 0.446	0.576	0.6	19.3368 \pm 0.0037	
GJ752 A*	169.1590 \pm 0.0520	-579.043 \pm 0.088	-1332.740 \pm 0.081	—	—	8.0976 \pm 0.0011	
GJ752 B	168.9620 \pm 0.1299	-598.177 \pm 0.245	-1365.270 \pm 0.227	0.855	98	14.3212 \pm 0.0007	1.4208 $^{+0.2795}_{-0.1719}$
HD 181234 A*	20.9155 \pm 0.0564	-122.751 \pm 0.098	-318.277 \pm 0.098	—	—	8.3693 \pm 0.0004	0.3670 $^{+0.1987}_{-0.0723}$
HD 181234 B	20.8683 \pm 0.1458	-117.558 \pm 0.192	-323.292 \pm 0.211	0.520	27	14.2207 \pm 0.0012	
Wendelstein-1 A*	3.2470 \pm 0.0317	4.131 \pm 0.041	-1.832 \pm 0.039	—	—	15.0324 \pm 0.0005	0.5240 $^{+0.4730}_{-0.4315}$
Wendelstein-1 B	3.5833 \pm 0.4053	3.862 \pm 0.508	-2.194 \pm 0.536	1.038	1.9	19.3979 \pm 0.0031	
2MJ2126-81 A*	29.2836 \pm 0.0690	59.843 \pm 0.111	-107.723 \pm 0.114	0.303	48	10.8133 \pm 0.0021	0.2157 $^{+0.4319}_{-0.0470}$ SHC
2MJ2126-81 B	29.2463 \pm 0.9205	56.511 \pm 1.656	-115.369 \pm 2.441	4.299	4.4	20.7247 \pm 0.0094	
TOI 132 A*	6.0809 \pm 0.0366	35.553 \pm 0.043	-53.055 \pm 0.054	0.090	3.6	11.3208 \pm 0.0007	0.1535 $^{+0.1606}_{-0.1430}$
TOI 132 B	5.9683 \pm 0.2251	35.417 \pm 0.280	-52.488 \pm 0.361	0.955	7.4	18.4470 \pm 0.0015	
NGTS-7 A*	7.2497 \pm 0.1203	-27.003 \pm 0.114	-16.225 \pm 0.178	0.610	72	14.9154 \pm 0.0020	0.5000 $^{+0.5000}_{-0.5000}$ ✖
NGTS-7 B	6.5232 \pm 0.0787	-28.601 \pm 0.112	-14.776 \pm 0.364	0.203	4.4	15.5134 \pm 0.0012	
DS Tuc A*	22.6663 \pm 0.0354	79.464 \pm 0.074	-67.440 \pm 0.045	—	—	8.3193 \pm 0.0010	
DS Tuc B	22.6504 \pm 0.0297	78.022 \pm 0.064	-65.746 \pm 0.037	—	—	9.3993 \pm 0.0014	0.3210 $^{+0.2350}_{-0.1034}$
IRXS J2351+3127 A*	23.2183 \pm 0.0524	106.584 \pm 0.064	-87.761 \pm 0.038	0.083	3.9	12.5145 \pm 0.0005	
IRXS J2351+3127 C	23.1794 \pm 0.0592	105.757 \pm 0.070	-87.787 \pm 0.041	0.285	32	13.2004 \pm 0.0006	0.4190 $^{+0.4250}_{-0.0410}$

Comments on individual objects:

- **HD 1160 A** hosts a brown dwarf companion (HD 1160 B, detected by Nielsen et al., 2012), which is listed as exoplanet in the EPE.
- The exoplanet host star **HD 24085 B** is the secondary component of a binary system, whose primary star HD 24085 A is also known as HD 24062.
- **HII 1348 A** is a spectroscopic binary with a brown dwarf companion (HII 1348 B, discovered by Geißler et al., 2012), which is listed as exoplanet in the EPE.
- **DH Tau A** hosts a brown dwarf companion (DH Tau B), which was detected by Itoh et al. (2005) and is listed as exoplanet in the EPE. DH Tau C (alias DI Tau) is the wide primary component of this system.
- **2M 0441+23 C** is an exoplanet host brown dwarf (Bowler and Hillenbrand, 2015), which is listed in the EPE.
- The bright AGB star **L2 Pup A** is listed in the Gaia DR2 but with a parallax ($\pi = 7.3644 \pm 0.6149$ mas) that significantly differs from its HIPPARCOS-value ($\pi = 15.61 \pm 0.99$ mas, van Leeuwen, 2007). Furthermore, it should be noted that the G-band brightness of this star, as listed in the Gaia DR2, is several magnitudes fainter than expected (e.g. $G = 3.97 \pm 0.54$ mag, as estimated by Smart and Nicastrò, 2014). Therefore, we only use here the Gaia DR2 equatorial coordinates of this star, while we adopt the HIPPARCOS-values of its parallax and proper motion, which is indicated with the flag HIP in this table.
- **HIP 73990 A** is the host star of two brown dwarfs (HIP 73990 B & C, revealed by Hinkley et al., 2015), which are both listed as exoplanets in the EPE.
- **GQ Lup A** is listed as exoplanet host star in the EPE, whose substellar companion was detected by Neuhäuser et al. (2005). The star exhibits a wide stellar companion, whose WDS designation (GQ Lup C) is used here.
- **HIP 79098 A** is a spectroscopic binary and hosts the brown dwarf HIP 79098 B (Janson et al., 2019), which is listed as exoplanet in the EPE.
- **ROXs 12 A** is the host star of the brown dwarf ROXs 12 B, detected by Kraus et al. (2014), which is listed as exoplanet in the EPE.
- **RXSJ2351+3127 A** hosts a brown dwarf companion (RXSJ2351+3127 B, discovered by Bowler et al., 2012), which is listed as exoplanet in the EPE.

-
- **HII 1348 A, FU Tau A, G 196-3 A, 2M J1155-7919 A, HD 97334 A, β Cir A, HIP 77900 A, USco 1602-2401 A, USco 1610-1913 A, USco 1612-1800 A, and 2M J2126-81 A**, are all listed as exoplanet host stars in the EPE, whose substellar companions were detected and characterized in this study, using data from the Gaia DR2.
 - **2M J1101-7732 A, 2M J1450-7841 A, 2M 1510 A** are all brown dwarfs, which are listed as exoplanet hosts in the EPE, whose substellar companions were detected and characterized in this study with Gaia DR2 data.

Table 3. The relative astrometry and WDS status of all detected companions.

Companion	ρ [arcsec]	PA [$^{\circ}$]	$\Delta\pi$ [mas]	$sig\text{-}\Delta\pi$	μ_{rel} [mas/yr]	$sig\text{-}\mu_{rel}$	$cpm\text{-}index$	not in WDS
HD 1160 C	5.14549 ± 0.00018	349.53223 ± 0.00259	0.95 ± 0.28	$3.3 (1.2)$	1.72 ± 0.33	5.2	30	
Gliese 49 B	294.45989 ± 0.00011	75.52728 ± 0.00002	0.17 ± 0.09	$2.0 (0.8)$	4.36 ± 0.23	19	338	
HD 8326 B	56.88131 ± 0.00005	147.16909 ± 0.00006	0.12 ± 0.08	$1.6 (0.3)$	1.18 ± 0.17	7.1	394	
HD 13167 B	20.06421 ± 0.00010	24.77589 ± 0.00028	0.11 ± 0.13	$0.8 (0.2)$	1.28 ± 0.23	5.7	91	★
HR 858 B	8.35742 ± 0.00013	15.79337 ± 0.00060	1.04 ± 0.18	$5.8 (1.2)$	13.90 ± 0.22	62	24	★ ¹
HD 18015 B	7.08916 ± 0.00006	316.16832 ± 0.00045	0.11 ± 0.07	$1.6 (1.6)$	1.61 ± 0.11	14	79	
K2-288 A	0.78692 ± 0.00018	340.38240 ± 0.01437	0.93 ± 0.22	$4.3 (1.0)$	4.75 ± 0.64	7.4	84	★ ²
HD 23472 B	9.56924 ± 0.00008	45.28294 ± 0.00046	0.08 ± 0.08	$1.1 (0.2)$	1.23 ± 0.18	7.0	181	★
HD 24085 A	75.91260 ± 0.00003	263.05666 ± 0.00002	0.04 ± 0.03	$1.3 (1.3)$	1.01 ± 0.06	16	194	★
HII 1348 C	36.02849 ± 0.00016	276.87735 ± 0.00017	0.34 ± 0.18	$1.9 (0.7)$	1.22 ± 0.35	3.5	82	★
HII 1348 D	55.01726 ± 0.00090	182.06892 ± 0.00182	0.91 ± 1.78	$0.5 (0.3)$	4.00 ± 3.05	1.3	25	★
HATS-57 B	14.44086 ± 0.00010	282.25351 ± 0.00032	0.06 ± 0.13	$0.4 (0.4)$	0.88 ± 0.16	5.4	43	★
FU Tau B	5.68952 ± 0.00112	123.57637 ± 0.00858	0.11 ± 1.30	$0.1 (0.0)$	5.60 ± 4.05	1.4	8	
DH Tau C	15.29981 ± 0.00007	126.08805 ± 0.00023	0.01 ± 0.09	$0.2 (0.2)$	0.53 ± 0.11	4.7	83	
51 Eri B (SB)	66.96749 ± 0.00027	162.62918 ± 0.00028	4.39 ± 0.39	$11.2 (2.1)$	19.04 ± 0.71	27	8	
2M 0441+23 AB	12.31449 ± 0.00036	57.55273 ± 0.00133	0.29 ± 0.39	$0.7 (0.2)$	0.67 ± 0.94	0.7	70	
NGTS-6 B	5.36108 ± 0.00005	116.68846 ± 0.00060	0.01 ± 0.07	$0.1 (0.0)$	0.14 ± 0.12	1.2	342	★
AB Dor BD	8.87930 ± 0.00018	347.19358 ± 0.00097	1.71 ± 0.17	$10.1 (1.7)$	53.56 ± 0.33	164	6	
HD 39855 B	10.72622 ± 0.00004	19.55064 ± 0.00017	0.00 ± 0.05	$0.0 (0.0)$	13.00 ± 0.09	145	15	
NGTS-10 B	1.12234 ± 0.00023	334.73644 ± 0.01107	2.78 ± 0.27	$10.2 (1.3)$	1.48 ± 0.41	3.6	14	★ ³
L2 Pup B	32.80132 ± 0.00052	63.66528 ± 0.00099	0.80 ± 0.99	$0.8 (-)$	2.32 ± 1.08	2.2	296	★
HIP 38594 B	399.81589 ± 0.00012	208.91546 ± 0.00001	0.06 ± 0.09	$0.7 (0.7)$	6.44 ± 0.24	27	113	
WASP-180 B	4.86185 ± 0.00006	138.92126 ± 0.00081	0.05 ± 0.09	$0.5 (0.5)$	1.42 ± 0.19	7.6	19	
HD 79211 A	17.08255 ± 0.00004	277.72812 ± 0.00014	0.01 ± 0.06	$0.1 (0.1)$	94.92 ± 0.08	1136	35	
HD 85628 B	4.33622 ± 0.00004	224.93946 ± 0.00056	0.12 ± 0.05	$2.5 (0.4)$	2.15 ± 0.08	27	14	★ ⁴
TOI 717 B	65.46692 ± 0.00016	88.63021 ± 0.00020	0.01 ± 0.11	$0.1 (0.1)$	2.10 ± 0.25	8.4	64	
G 196-3 B	16.06941 ± 0.00055	209.15563 ± 0.00166	1.51 ± 0.81	$1.9 (0.6)$	6.99 ± 1.53	4.6	71	
LTT 3780 B	15.78849 ± 0.00011	97.14133 ± 0.00038	0.18 ± 0.14	$1.3 (0.4)$	0.55 ± 0.17	3.2	1535	
MASCARA-3 B	2.06449 ± 0.00010	173.15273 ± 0.00345	0.69 ± 0.13	$5.3 (0.9)$	6.20 ± 0.31	20	21	★ ⁵
2M J101-7732 B	1.42656 ± 0.00041	30.00553 ± 0.01621	0.03 ± 0.39	$0.1 (0.0)$	1.02 ± 0.86	1.2	45	
WASP-175 B	7.25020 ± 0.00003	4.95541 ± 0.00027	0.03 ± 0.05	$0.6 (0.6)$	0.29 ± 0.07	3.9	175	★ ⁶

Table 3. continued

Companion	ρ [arcsec]	PA [$^{\circ}$]	$\Delta\pi$ [mas]	$sig-$ $\Delta\pi$	μ_{rel} [mas/yr]	$sig-$ μ_{rel}	$cpm-$ $index$	not in WDS
CHXR 73 C	46.10344 \pm 0.00027	248.30821 \pm 0.00031	0.02 \pm 0.28	0.1 (0.0)	1.65 \pm 0.42	3.9	27	★
GJ 414 B	34.15873 \pm 0.00007	262.44625 \pm 0.00011	0.12 \pm 0.07	1.6 (1.6)	16.09 \pm 0.12	139	78	
HD 97334 BC	89.88421 \pm 0.00098	245.04583 \pm 0.00060	1.27 \pm 1.10	1.2 (0.2)	13.05 \pm 2.13	6.1	44	
HD 233832 B	4.93691 \pm 0.00004	266.38672 \pm 0.00079	0.07 \pm 0.09	0.8 (0.8)	6.88 \pm 0.11	63	143	
2M J1155-7919 B	5.75435 \pm 0.00047	227.86140 \pm 0.00458	0.07 \pm 0.53	0.1 (0.0)	1.48 \pm 1.20	1.2	55	★ ⁷
NGTS-5 B	26.89147 \pm 0.00011	116.31597 \pm 0.00021	0.29 \pm 0.13	2.2 (0.7)	0.46 \pm 0.20	2.3	63	★
2M J1450-7841 B	4.23901 \pm 0.00099	313.26065 \pm 0.01318	2.29 \pm 1.03	2.2 (0.7)	3.01 \pm 2.17	1.4	29	★ ⁸
WASP-189 B	9.41610 \pm 0.00010	70.78901 \pm 0.00095	0.72 \pm 0.18	4.0 (1.4)	0.25 \pm 0.21	1.2	446	★
HIP 73990 D	47.27427 \pm 0.00009	56.65125 \pm 0.00010	0.08 \pm 0.11	0.7 (0.2)	0.37 \pm 0.18	2.0	219	★
TOI 905 B	2.24803 \pm 0.00050	100.34253 \pm 0.01658	1.58 \pm 0.55	2.9 (1.0)	7.67 \pm 0.76	10	12	
2M 1510 B	6.77139 \pm 0.00046	209.28499 \pm 0.00431	0.47 \pm 0.56	0.8 (0.2)	1.74 \pm 0.95	1.8	146	★ ⁹
β Cir B	217.62247 \pm 0.00055	199.25875 \pm 0.00013	0.39 \pm 0.81	0.5 (0.1)	4.29 \pm 1.08	4.0	78	
KELT-23 B	4.54135 \pm 0.00006	127.68919 \pm 0.00069	0.00 \pm 0.06	0.1 (0.0)	1.18 \pm 0.10	1.2	21	★ ¹⁰
K2-290 C	11.25119 \pm 0.00017	179.97609 \pm 0.00151	0.42 \pm 0.28	1.5 (0.7)	0.47 \pm 0.44	1.1	135	★ ¹¹
GQ Lup C	16.11286 \pm 0.00039	114.61327 \pm 0.00099	1.09 \pm 0.46	2.4 (0.4)	1.74 \pm 0.70	2.5	31	
HIP 77900 B	22.27990 \pm 0.00044	12.74996 \pm 0.00267	1.38 \pm 0.98	1.4 (0.6)	2.08 \pm 1.14	1.8	27	★ ¹²
USco 1602-2401 B	7.21512 \pm 0.00008	353.20771 \pm 0.00157	0.61 \pm 0.21	2.9 (0.7)	0.86 \pm 0.34	2.5	62	
HIP 79098 C	65.29721 \pm 0.00018	101.86730 \pm 0.00008	0.35 \pm 0.19	1.9 (0.5)	2.30 \pm 0.28	8.3	25	★ ¹³
USco 1610-1913 B	5.82725 \pm 0.00040	113.57990 \pm 0.00238	0.54 \pm 0.38	1.4 (0.4)	2.69 \pm 1.01	2.7	19	
USco 1612-1800 B	3.18438 \pm 0.00019	10.65437 \pm 0.00561	0.27 \pm 0.33	0.8 (0.2)	1.47 \pm 0.54	2.7	29	★ ¹⁴
ROXs 12 C	37.14026 \pm 0.00004	185.99483 \pm 0.00012	0.06 \pm 0.08	0.7 (0.1)	0.66 \pm 0.17	3.9	79	★ ¹⁵
HATS-48 B	5.43813 \pm 0.00025	267.59024 \pm 0.00322	0.13 \pm 0.44	0.3 (0.2)	0.96 \pm 0.45	2.2	13	★ ¹⁶
GJ 752 B	75.48951 \pm 0.00011	152.49075 \pm 0.00009	0.20 \pm 0.14	1.4 (0.2)	37.74 \pm 0.25	153	78	
HD 181234 B	5.17023 \pm 0.00011	56.61253 \pm 0.00118	0.05 \pm 0.16	0.3 (0.1)	7.22 \pm 0.22	32	95	
Wendelstein-1 B	11.79208 \pm 0.00024	232.62838 \pm 0.00116	0.34 \pm 0.41	0.8 (0.3)	0.45 \pm 0.53	0.9	20	★
2M J2126-81 B	217.49441 \pm 0.00082	123.98914 \pm 0.00024	0.04 \pm 0.92	0.0 (0.0)	8.34 \pm 2.34	3.6	30	
TOI 132 B	19.64887 \pm 0.00018	151.44437 \pm 0.00044	0.11 \pm 0.23	0.5 (0.1)	0.58 \pm 0.36	1.6	218	★
NGTS-7 B	1.13095 \pm 0.00014	117.57142 \pm 0.01072	0.73 \pm 0.14	5.1 (1.1)	2.16 \pm 0.30	7.3	30	★ ¹⁷
DS Tuc B	5.36461 \pm 0.00003	347.65815 \pm 0.00047	0.02 \pm 0.05	0.3 (0.3)	2.22 \pm 0.08	29	93	
IRXS J2351+3127 C	126.01641 \pm 0.00005	98.50769 \pm 0.00002	0.04 \pm 0.08	0.5 (0.1)	0.83 \pm 0.09	8.7	333	

Comments on individual companions:

- 1: This companion was first reported by Vanderburg et al. (2019), who have already verified its equidistance and common proper motion with the exoplanet host star HR 858 A using Gaia DR2 data, consistent with the results, obtained in this study.
- 2: This companion was detected by Feinstein et al. (2019) and its companionship with the exoplanet host star K2-288 B was proven with Gaia DR2 astrometry, confirmed by the astrometric analysis, carried out in the study, presented here.
- 3: This star was already noticed in the Gaia DR2 by McCormac et al. (2020) as common proper motion companion of the exoplanet host star NGTS-10 A, consistent with the results, derived in this study.
- 4: This companion of the exoplanet host star HD 85628 A was discovered by Dorval et al. (2020) in the Gaia DR2, who found its parallax and proper motion consistent with that of the exoplanet host star, confirmed by the astrometric analysis, presented here.
- 5: This companion was detected with AO imaging by Rodriguez et al. (2019) using Keck/NIRC 2, but is also listed in the Gaia DR2, whose astrometry was used by this team to verify the equidistance and common proper motion of this companion with the exoplanet host star MASCARA-3 A, as done in this study.
- 6: This companion was already reported by Nielsen et al. (2019), who proved its companionship with the exoplanet host star WASP-175 A with Gaia DR2 astrometry, consistent with the results derived here.
- 7: The equidistance and common proper motion of this substellar object with the exoplanet host star 2MJ1155-7919 A was verified by Dickson-Vandervelde et al. (2020) using Gaia DR2 data, as done in this work.
- 8: This companion was detected by Burgasser et al. (2017) and its common proper motion with the brown dwarf 2MJ1450-7841 A, listed in the EPE, was verified with ground based astrometry, confirmed in this study with Gaia DR2 data, which furthermore proves the equidistance of both objects.
- 9: This companion was noticed by Triaud et al. (2020) in the Gaia DR2 as equidistant and co-moving companion of the brown dwarf 2M 1510 A, which is listed in the EPE, consistent with our results.
- 10: KELT-23 B was first discovered by (Johns et al., 2019) with Keck/NIRC 2 AO imaging, who used Gaia DR2 astrometry to prove the equidistance and common proper motion of the companion with the exoplanet host star KELT-23 A, as done in this study.
- 11: This companion was already described by Hjorth et al. (2019), who have verified it to be equidistant and co-moving with the exoplanet host star K2-290 A, using Gaia DR2 data, a conclusion, which is confirmed by the analysis, presented here. Furthermore, this team identified an additional but closer stellar companion-candidate of the exoplanet host star (K2-290 B) with Subaru/IRCS AO imaging, which however still needs astrometric confirmation of its companionship. Due to its close angular separation to K2-290 A we adopt here this object as companion of the exoplanet host star.
- 12: This companion was revealed spectro-photometrically by Aller et al. (2013). With Gaia DR2 astrometry we prove here its companionship with the exoplanet host star HIP 77900 A.
- 13: HIP 79098 C was reported by (Janson et al., 2019) as equidistant and co-moving companion of the exoplanet host star HIP 79098 A, based on its Gaia DR2 astrometry, confirmed by the analysis of the companion, which is presented here.

- 14: This companion was revealed spectro-photometrically by Aller et al. (2013). The equidistance and common proper motion of this companion with the exoplanet host star USco 1612-1800 A was proven in this study, with Gaia DR2 astrometry.
- 15: This star was identified by (Bowler et al., 2017) as companion of ROXs 12 A, based on its radial velocity and proper motion. We prove the equidistance of both stars with their Gaia DR2 astrometry, which also confirms their common proper motion.
- 16: This companion was reported by (Hartman et al., 2020), who used the Gaia DR2 astrometry to confirm its companionship with the exoplanet host star HATS-48 A, as done in this work.
- 17: NGTS-7 B was revealed by (Jackman et al., 2019) as companion of the exoplanet host star NGTS-7 A using Gaia DR2 astrometry, as done in this study.

Table 4. The equatorial coordinates and derived physical properties of all detected companions.

Companion	α [°]	δ [°]	M_G [mag]	sep [au]	$mass$ [M_\odot]	T_{eff} [K]	Flags
HD 1160 C	3.98858470355	4.25245524714	9.72 ^{+0.10} _{-0.13}	648	0.378 ^{+0.021} _{-0.016}	3503 ⁺²⁵ ₋₁₉	BPRP PRI
Gliese 49 B	15.83942593995	62.36588062663	11.35 ^{+0.41} _{-0.22}	2902	0.169 ^{+0.020} _{-0.030}	3211 ⁺⁴⁰ ₋₇₄	2MA BPRP PRI
HD 8326 B	20.54104760211	-26.90734439784	11.48 ^{+0.04} _{-0.25}	1747	0.198 ^{+0.023} _{-0.003}	3257 ⁺³⁷ ₋₇	2MA BPRP PRI
HD 13167 B	32.06020575541	-24.69051459458	11.33 ^{+0.07} _{-0.06}	3001	0.211 ^{+0.006} _{-0.007}	3279 ⁺⁹ ₋₁₀	2MA BPRP
HR 858 B	42.98571355919	-30.81182706733	13.39 ^{+0.09} _{-0.11}	267	0.112 ^{+0.003} _{-0.002}	2926 ⁺²⁰ ₋₁₉	BPRP PRI
HD 18015 B	43.36225373946	-8.84661863284	6.62 ^{+0.04} _{-0.04}	881	0.747 ^{+0.004} _{-0.004}	4650 ⁺²⁰ ₋₁₈	2MA BPRP PRI
K2-288 A	55.44420842474	18.26869720107	8.65 ^{+0.09} _{-0.09}	52	0.534 ^{+0.010} _{-0.010}	3777 ⁺³⁰ ₋₂₈	2MA
HD 23472 B	55.46315889099	-62.76539647729	12.79 ^{+0.07} _{-0.39}	374	0.129 ^{+0.006} _{-0.002}	3038 ⁺³⁰ ₋₁₃	2MA BPRP PRI
HD 24085 A	56.19506729271	-70.02706843481	2.90 ^{+0.39} _{-0.59}	4174	1.254 ^{+0.088} _{-0.058}	6339 ⁺²¹¹ ₋₁₃₉	2MA BPRP PRI EXT
HII 1348 C	56.81444339267	24.39176993016	10.07 ^{+0.33} _{-0.31}	5155	0.322 ^{+0.048} _{-0.046}	3436 ⁺⁵⁸ ₋₆₀	2MA BPRP PRI ***
HII 1348 D	56.82474725542	24.37529892928	14.35 ^{+0.46} _{-0.37}	7872	0.055 ^{+0.005} _{-0.006}	2602 ⁺⁷⁸ ₋₉₆	BD 2MA BPRP ***
HATS-57 B	60.94413061754	-19.05596683949	10.25 ^{+0.05} _{-0.18}	4068	0.331 ^{+0.023} _{-0.007}	3448 ⁺²⁴ ₋₇	2MA BPRP
FU Tau B	65.89894960541	25.04979704793	12.62 ^{+0.49} _{-0.26}	749	0.018 ^{+0.002} _{-0.003}	2553 ⁺³⁸ ₋₇₁	BD 2MA BPRP
DH Tau C	67.42700661202	26.54688636442	3.64 ^{+0.17} _{-0.37}	2071	1.655 ^{+0.228} _{-0.106}	4837 ⁺¹⁶⁴ ₋₇₇	2MA BPRP PRI EXT
51 Eri B (SB)	69.40630139702	-2.49157819607	7.18 ^{+0.11} _{-0.27}	1994	0.733 ^{+0.056} _{-0.024}	3962 ⁺¹¹⁶ ₋₄₉	2MA BPRP PRI ***
2M 0441+23 AB ¹	70.44024465438	23.03268965375	7.37 ^{+0.43} _{-0.96}	1483	0.241 ^{+0.147} _{-0.061}	3308 ⁺³⁰⁰ ₋₁₃₈	2MA BPRP
NGTS-6 B	75.79692465277	-30.40013000839	9.23 ^{+0.14} _{-0.10}	1667	0.457 ^{+0.013} _{-0.018}	3618 ⁺²¹ ₋₂₉	2MA BPRP PRI
AB Dor BD	82.18603484814	-65.44557858318	9.08 ^{+0.44} _{-0.52}	136	0.466 ^{+0.061} _{-0.059}	3645 ⁺¹⁶⁷ ₋₁₀₄	2MA BPRP PRI ***
HD 39855 B	88.62713212305	-19.70163948841	8.02 ^{+0.13} _{-0.23}	250	0.598 ^{+0.024} _{-0.014}	3978 ⁺¹⁰³ ₋₄₁	2MA BPRP PRI
NGTS-10 B	91.87213254706	-25.59461438962	7.27 ^{+0.61} _{-1.21}	364	0.665 ^{+0.121} _{-0.059}	4327 ⁺⁶⁰⁶ ₋₂₈₄	
L2 Pup B	108.39678197580	-44.63427669967	11.39 ^{+0.17} _{-0.33}	2101	0.203 ^{+0.032} _{-0.012}	3270 ⁺⁴⁹ ₋₂₆	
HIP 38594 B	118.48449010900	-25.39952189079	14.43 ^{+0.26} _{-0.78}	7116	~ 0.6		WD 2MA BPRP PRI
WASP-180 B	123.39313443835	-1.98380547425	4.64 ^{+0.06} _{-0.16}	1244	1.057 ^{+0.029} _{-0.011}	5778 ⁺⁹³ ₋₃₆	2MA BPRP PRI
HD 79211 A	138.58391575741	52.68415915741	7.59 ^{+0.21} _{-0.33}	108	0.644 ^{+0.034} _{-0.022}	4180 ⁺¹⁵³ ₋₉₇	2MA BPRP PRI

Table 4. continued

Companion	α [°]	δ [°]	M_G [mag]	sep [au]	$mass$ [M_\odot]	T_{eff} [K]	Flags
HD 85628 B	147.57796550484	-66.11477795490	$7.38^{+0.23}_{-0.15}$	744	$0.675^{+0.016}_{-0.025}$	4282^{+66}_{-104}	BPRP PRI
TOI 717 B	147.98872815946	2.11708155887	$9.72^{+0.02}_{-0.13}$	2275	$0.398^{+0.017}_{-0.003}$	3519^{+25}_{-3}	2MA BPRP PRI
G 196-3 B	151.08506490419	50.38228242112	$17.41^{+0.48}_{-0.49}$	350	$0.032^{+0.002}_{-0.002}$	1987^{+94}_{-93}	BD 2MA BPRP
LTT 3780 B	154.64934761666	-11.71834621199	$12.27^{+0.34}_{-0.26}$	347	$0.149^{+0.014}_{-0.014}$	3127^{+43}_{-58}	2MA BPR PPRI
MASCARA-3 B	161.90924448675	71.65515762432	$7.83^{+0.12}_{-0.28}$	200	$0.625^{+0.030}_{-0.013}$	4074^{+126}_{-53}	
2M J1101-7732 B	165.33045751133	-77.54374799758	$12.48^{+0.14}_{-0.14}$	264	$0.019^{+0.001}_{-0.001}$	2574^{+21}_{-21}	BD
WASP-175 B	166.31900970217	-34.12073886500	$5.46^{+0.10}_{-0.11}$	3971	$0.919^{+0.018}_{-0.016}$	5290^{+65}_{-60}	2MA BPR PPRI
CHXR 73 C	166.56385863699	-77.63060598303	$8.04^{+1.03}_{-1.03}$	8808	$0.235^{+0.148}_{-0.112}$	3280^{+295}_{-260}	2MA BPRP
GJ 414 B	167.76359381364	30.44392150823	$8.06^{+0.32}_{-0.57}$	406	$0.587^{+0.056}_{-0.034}$	3971^{+249}_{-110}	2MABPRP PRI
HD 97334 BC ²	168.10555672848	35.80289455668	$18.16^{+0.04}_{-0.19}$	2036	$0.028^{+0.001}_{-0.001}$	1845^{+36}_{-8}	BD 2MA BPRP
HD 233832 B	171.51750545565	50.37622350226	$8.64^{+0.11}_{-0.21}$	290	$0.531^{+0.022}_{-0.012}$	3775^{+68}_{-36}	2MA BPRP PRI
2M J1155-7919 B	178.76276748600	-79.32082818366	$14.48^{+0.02}_{-0.06}$	582	$0.016^{+0.001}_{-0.001}$	2366^{+10}_{-2}	BD 2MA BPRP
NGTS-5 B	221.06499706987	5.60206193982	$9.67^{+0.12}_{-0.11}$	8323	$0.405^{+0.014}_{-0.016}$	3530^{+22}_{-20}	2MA BPRP
2M J1450-7841 B	222.67064914833	-78.69407266366	$15.35^{+0.51}_{-0.51}$	387	$0.031^{+0.005}_{-0.003}$	2328^{+114}_{-100}	BD 2MA BPRP
WASP-189 B	225.68920534342	-3.03062676806	$9.12^{+0.23}_{-0.16}$	942	$0.479^{+0.021}_{-0.030}$	3646^{+33}_{-48}	2MA BPRP PRI
HIP 73990 D	226.82470360183	-29.49738818566	$8.33^{+0.45}_{-0.64}$	5234	$0.470^{+0.151}_{-0.098}$	3576^{+191}_{-107}	2MA BPRP PRI
TOI 905 B	227.66059753260	-71.36174373792	$10.93^{+0.17}_{-0.14}$	358	$0.251^{+0.014}_{-0.016}$	3340^{+21}_{-25}	
2M 1510 B	227.69777941730	-28.30671294175	$15.13^{+0.03}_{-0.14}$	249	$0.033^{+0.001}_{-0.001}$	2376^{+31}_{-6}	BD 2MA BPRP
β Cir B	229.33920903332	-58.85886078926	$16.91^{+0.16}_{-0.23}$	6187	$0.063^{+0.002}_{-0.002}$	2159^{+47}_{-48}	BD 2MA BPRP
KELT-23 B	232.14912993468	66.35793842725	$9.94^{+0.05}_{-0.10}$	575	$0.368^{+0.014}_{-0.007}$	3487^{+15}_{-7}	2MA BPRP PRI
K2-290 C	234.85788601749	-20.20202286624	$10.51^{+0.27}_{-0.26}$	3094	$0.292^{+0.033}_{-0.026}$	3404^{+38}_{-41}	2MA BPRP ***
GQ Lup C	237.30537201266	-35.65336961027	$9.70^{+0.42}_{-0.34}$	2446	$0.075^{+0.016}_{-0.015}$	2897^{+14}_{-33}	2MA BPRP
HIP 77900 B	238.62692763313	-27.33270712891	$13.48^{+0.05}_{-0.16}$	3374	$0.020^{+0.001}_{-0.001}$	2519^{+22}_{-8}	BD BPRP
USco 1602-2401 B ³	240.71312906858	-24.03074240242	$8.69^{+0.12}_{-0.12}$	1038	$0.238^{+0.016}_{-0.017}$	3280^{+25}_{-27}	2MA BPRP PRI

Table 4. continued

Companion	α [°]	δ [°]	M_G [mag]	sep [au]	$mass$ [M_\odot]	T_{eff} [K]	Flags
HIP 79098 C	242.20150369275	-23.68925441843	$9.82^{+0.24}_{-0.15}$	9555	$0.159^{+0.013}_{-0.020}$	3176^{+24}_{-40}	2MA BPRP PRI ***
USco 1610-1913 B	242.63466253957	-19.21910506083	$12.71^{+0.39}_{-0.39}$	777	$0.025^{+0.003}_{-0.003}$	2615^{+47}_{-47}	BD 2MA BPRP
USco 1612-1800 B	243.20402838620	-18.01380384763	$12.50^{+0.39}_{-0.39}$	504	$0.026^{+0.003}_{-0.003}$	2642^{+48}_{-48}	BD BPRP
ROXs 12 C	246.61560598363	-25.45695531769	$7.28^{+1.00}_{-1.00}$	5095	$0.474^{+0.259}_{-0.181}$	3657^{+343}_{-289}	2MA BPR PPRI
HATS 48 B	288.66902407326	-59.57941400923	$11.71^{+0.37}_{-0.19}$	1444	$0.181^{+0.013}_{-0.022}$	3219^{+30}_{-60}	2MA BPRP
GJ 752 B	289.23745710752	5.14456304678	$14.04^{+0.17}_{-0.28}$	446	$0.098^{+0.005}_{-0.002}$	2785^{+60}_{-36}	2MA BPRP PRI
HD 181234 B	290.00108472870	-9.32417966740	$10.46^{+0.07}_{-0.20}$	247	$0.297^{+0.026}_{-0.007}$	3412^{+29}_{-11}	2MA BPRP PRI
Wendelstein-1 B	299.04791069915	17.56797448132	$11.43^{+0.43}_{-0.47}$	3632	$0.202^{+0.047}_{-0.030}$	3264^{+72}_{-70}	2MA BPRP
2M J2126-81 B	321.71158783493	-81.67526360458	$17.84^{+0.05}_{-0.43}$	7427	$0.020^{+0.001}_{-0.004}$	1851^{+41}_{-77}	BD 2MA BPRP
TOI 132 B	338.40325545731	-43.44166603901	$12.21^{+0.14}_{-0.16}$	3231	$0.152^{+0.009}_{-0.006}$	3137^{+27}_{-24}	2MA BPRP
NGTS-7 B	352.52202473338	-38.97006605140	$9.32^{+0.50}_{-0.50}$	156	$0.384^{+0.097}_{-0.091}$	3495^{+102}_{-97}	
DS Tuc B	354.91457052896	-69.19458723114	$5.86^{+0.10}_{-0.24}$	237	$0.834^{+0.060}_{-0.027}$	5040^{+180}_{-79}	2MA BPRP PRI
1RXS J2351+3127 C	357.93142859121	31.45083817280	$9.61^{+0.04}_{-0.43}$	5427	$0.394^{+0.057}_{-0.007}$	3522^{+98}_{-8}	2MA BPRP PRI

Table Footnotes:

1: 2M 0441+23 B is a close brown dwarf companion of 2M 0441+23 A.

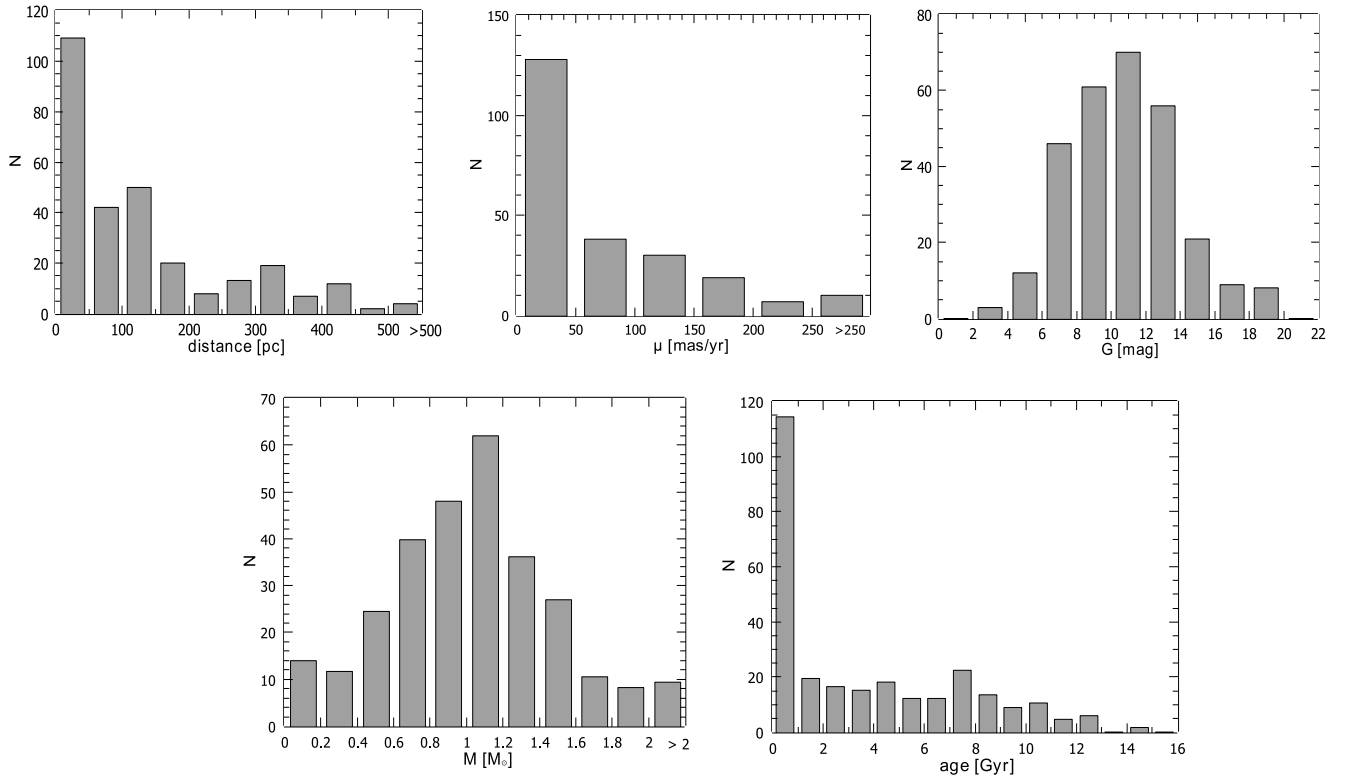
2: HD 97334 BC is a binary brown dwarf system.

3: The brown dwarf USco 1602-2401 B was detected by Aller et al. (2013) and its possible companionship to USco 1602-2401 A, was revealed with photometry and follow-up spectroscopy, which was finally proven in this study with the Gaia DR2 astrometry of the companion, i.e. confirmation of equidistance, and common proper motion, as well as test for gravitational stability. USco 1602-2401 B is one of 14 reported substellar companions, detected by Gaia, which were also characterized in this study using their Gaia DR2 astro- and photometry. In general, the derived mass of these substellar companions agrees well with the mass given in the literature, with a deviation of only a few M_{Jup} , on average. In contrast, for USco 1602-2401 B Aller et al. (2013) derived a mass of $41^{+20}_{-13} M_{Jup}$ at an age of 5 Myr ($47^{+20}_{-18} M_{Jup}$ at 10 Myr) adopting a distance of about 145 pc and no extinction. With the Gaia DR2 parallax and the Starhorse extinction estimate of the primary star and the G-band photometry of the companion we obtained a significantly higher mass of $0.238^{+0.016}_{-0.017} M_\odot$ at 5 Myr ($0.309^{+0.020}_{-0.019} M_\odot$ at 10 Myr). Adopting $A_G = 0$ mag yields a mass of the companion of $0.071^{+0.001}_{-0.001} M_\odot$ for 5 Myr, and $0.104^{+0.001}_{-0.001} M_\odot$ for 10 Myr, respectively. Therefore, we classify this companion here as low-mass star.

Table 5. List of all detected companions, whose differential proper motion μ_{rel} exceeds their estimated escape velocity μ_{esc} .

Companion	μ_{rel} [mas/yr]	μ_{esc} [mas/yr]	
51 Eri B (SB)	19.04 ± 0.71	11.298 ± 0.144	***
HIP 38594 B	6.44 ± 0.24	4.965 ± 0.082	
TOI 905 B	7.67 ± 0.76	3.090 ± 0.144	

6 FIGURES

**Figure 1.** The histograms of the individual properties of all targets of this study.

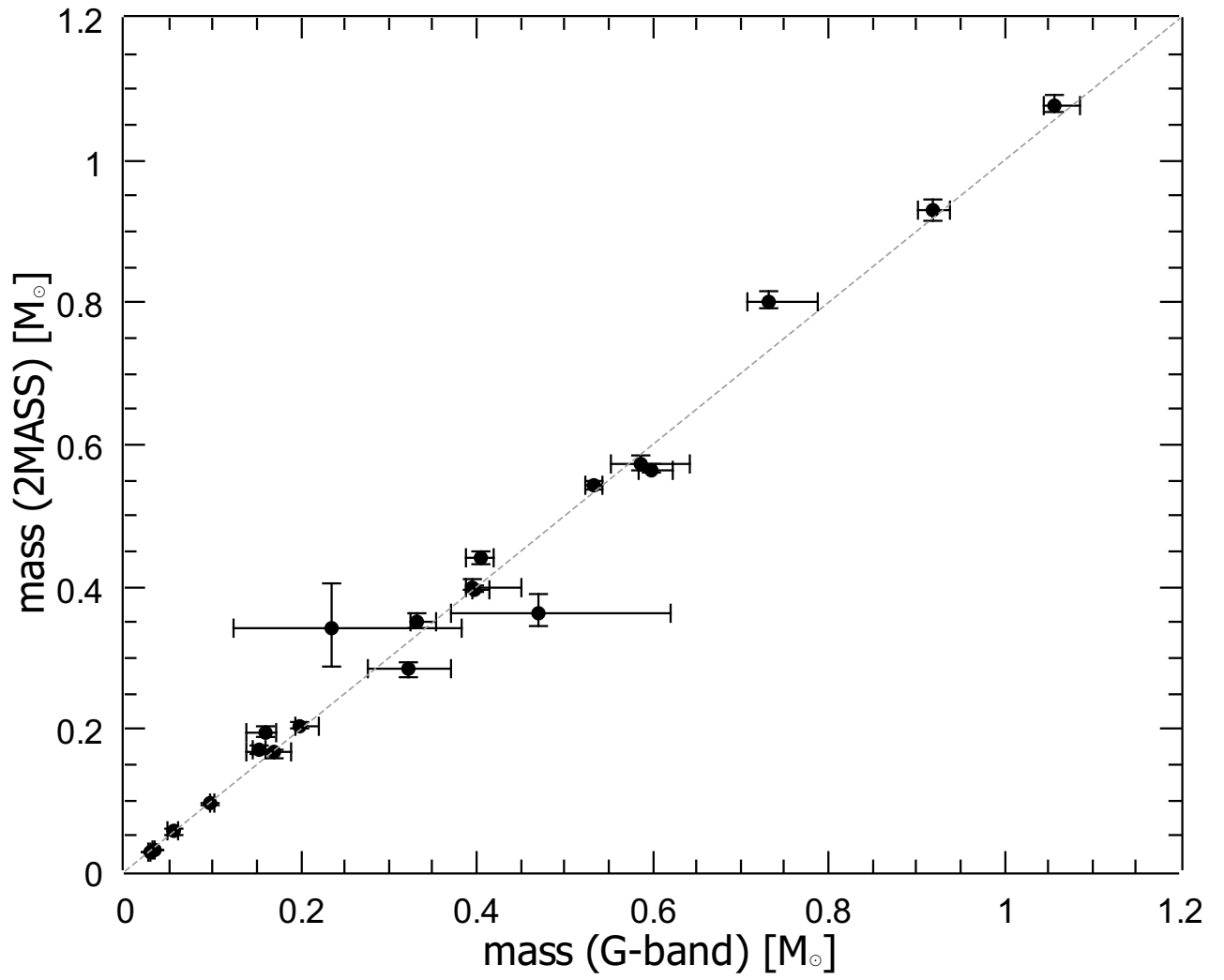


Figure 2. Comparison of the mass of the detected companions, derived from their G-band and infrared 2MASS photometry.

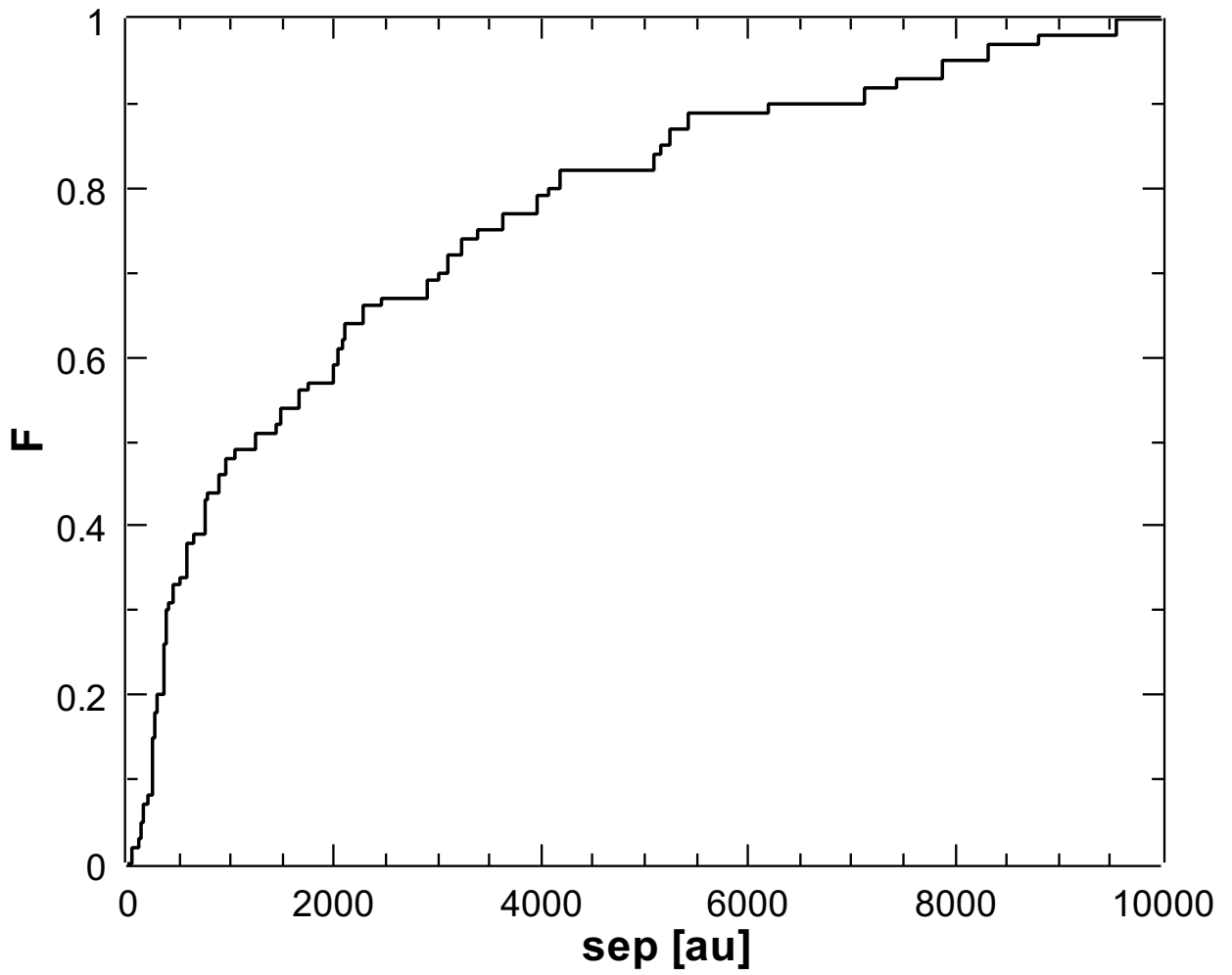


Figure 3. The cumulative distribution function of the projected separation (sep) of all detected companions to the associated exoplanet hosts.

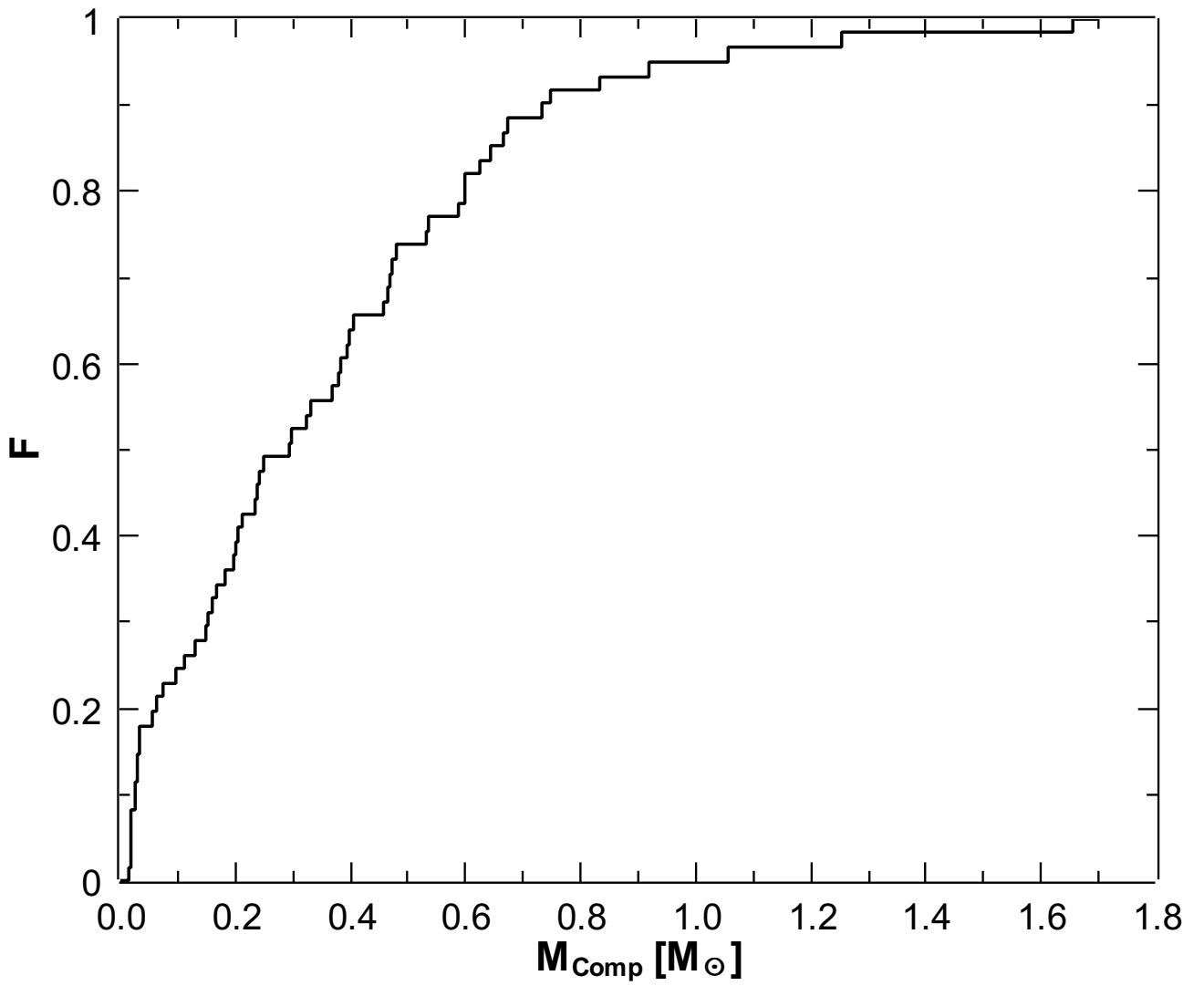


Figure 4. The cumulative distribution function of the mass of all companions, detected in this study.

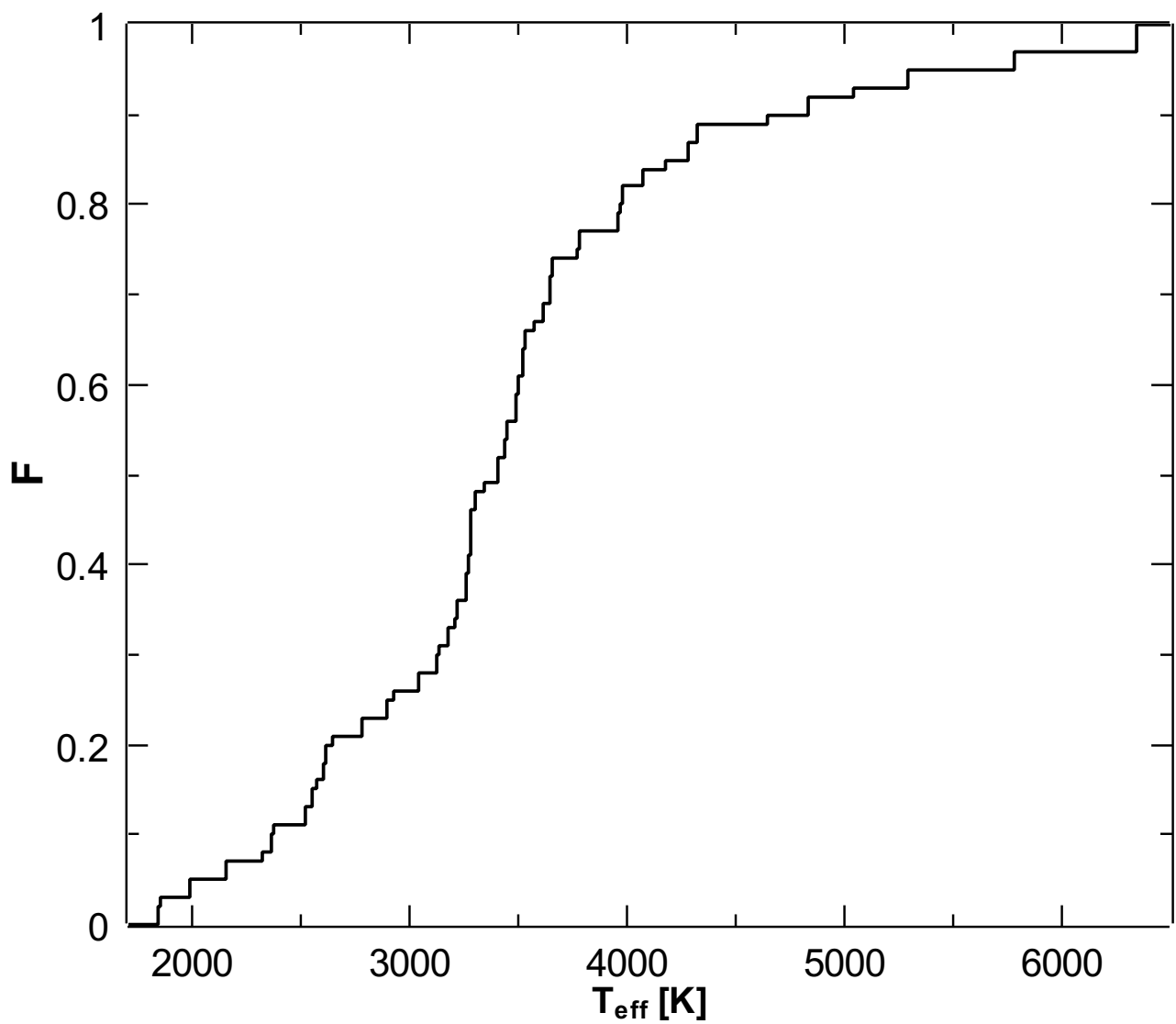


Figure 5. The cumulative distribution function of the effective temperature of all detected companions.

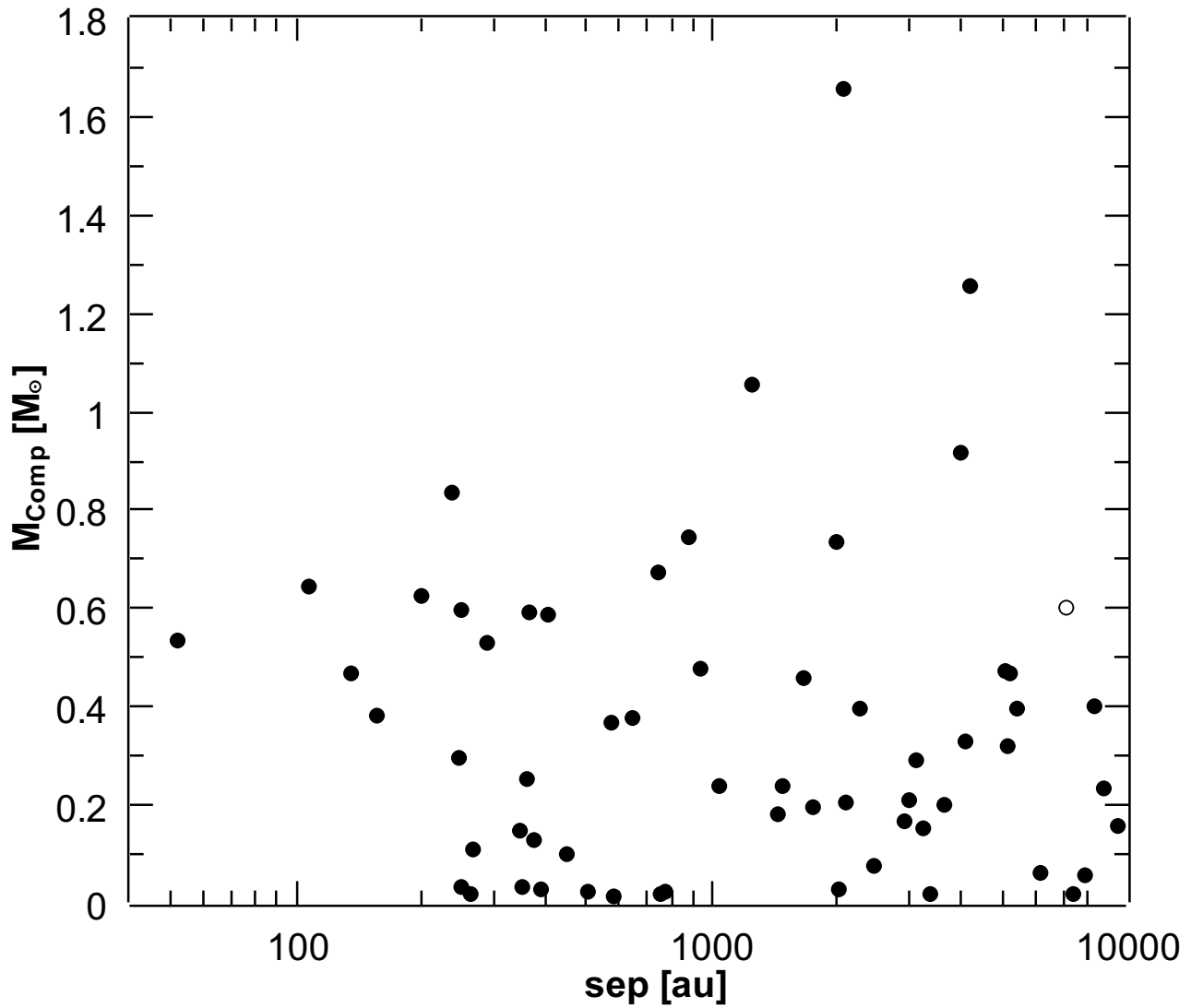


Figure 6. The mass of all companions, detected in this study, plotted over their projected separation (sep) to the associated exoplanet hosts. The white dwarf companion HIP 38594 B, is illustrated as open circle.

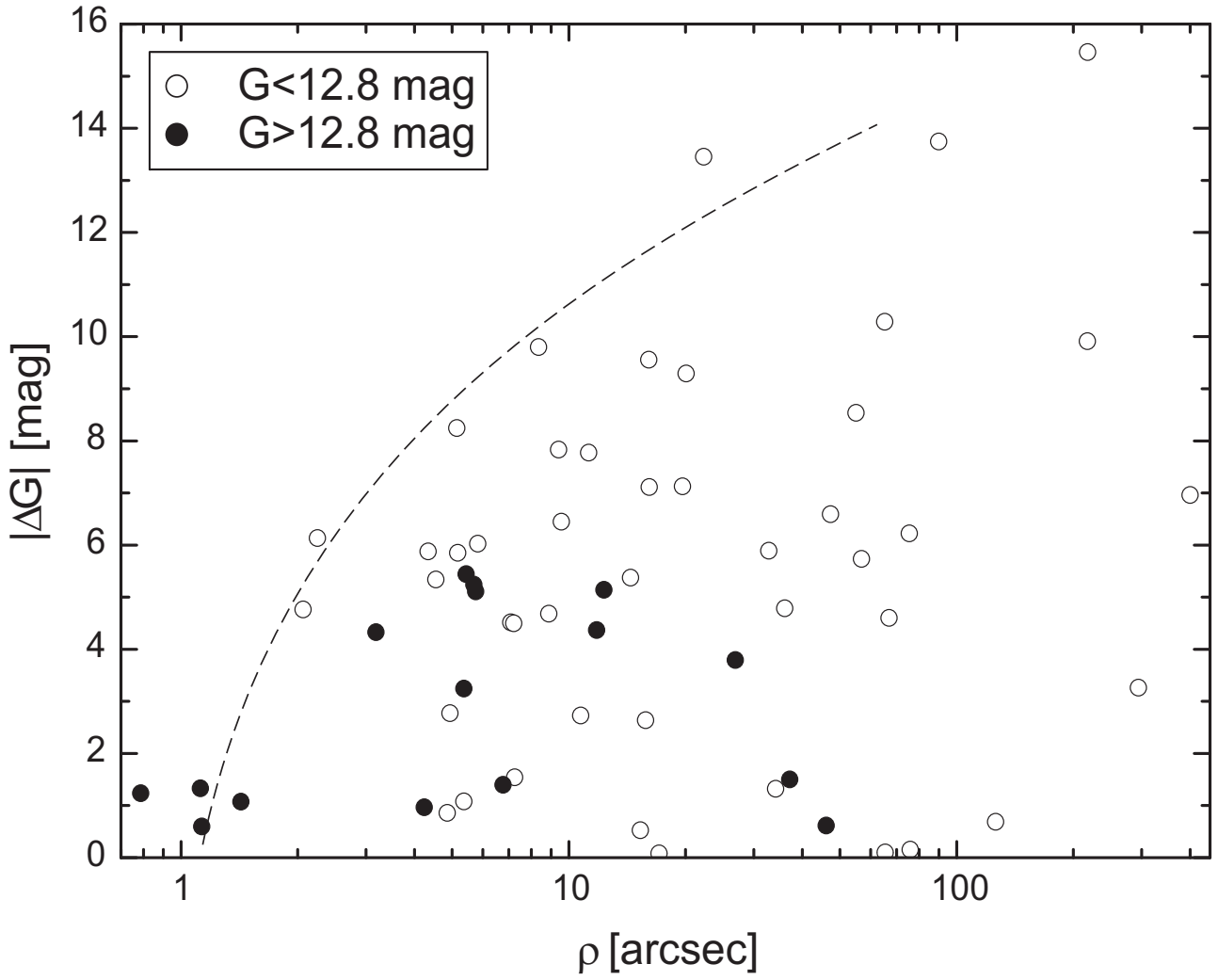


Figure 7. The G-band magnitude difference of all detected companions, plotted over their angular separation to the associated exoplanet hosts.